Further Characterization of the Spin Coupling Observed in Oxidized Hydrogenase from *Chromatium vinosum.* A Mössbauer and Multifrequency EPR Study†

Kristene K. Surerus,‡,§ Min Chen,‖ J. Wim van der Zwaan,‖ Frank M. Rusnak,⊥ Michael Kolk,‖ Evert C. Duin,‖ Simon P. J. Albracht,¶ and Eckard Münck*,‡

Department of Chemistry, Carnegie Mellon University, 4400 Fifth Avenue, Pittsburgh, Pennsylvania 15213-3890, E. C. Slater Institute, Laboratory of Biochemistry, University of Amsterdam, Plantage Muidergracht 12, NL-1018 TV Amsterdam, The Netherlands, and Department of Hematology Research, Mayo Clinic and Foundation, Rochester, Minnesota 55905

Received November 16, 1993; Revised Manuscript Received February 15, 1994®

ABSTRACT: Hydrogenase from *Chromatium vinosum* contains 1 Ni, 11-12 Fe, and ca. 9 sulfides. EPR and Mössbauer studies of the enzyme prepared in four different oxidation states show that the enzyme contains two Fe_4S_4 and one Fe_3S_4 cluster. In the oxidized (2+) state, the Mössbauer parameters of the two Fe_4S_4 clusters are typical for this cluster type. Upon reduction, however, these clusters do not exhibit the familiar $g = 1.94$ signal. The unusual nature of the reduced clusters is also borne out by the Mössbauer spectra which exhibit fairly small magnetic hyperfine interactions similar to those of centers I and II of the *Desulfovibrio gigas* enzyme. The Mössbauer spectra of the Fe_3S_4 cluster in the oxidized (1+) and reduced states are typical for this cluster type. The *C. vinosum* hydrogenase undergoes a reversible redox reaction at $E_m = +150$ mV (vs NHE). Above +150 mV the EPR spectra exhibit signals (previously called signals 2 and 4) that reflect a weak interaction between Ni(III) and an Fe-containing moiety. By clamping the Ni in the diamagnetic Ni(II)·CO form, we have discovered that signal 2 (X-band resonances at $g = 2.01$, 1.974, and 1.963) involves the Fe_3S_4 cluster and an as yet unidentified paramagnetic moiety. The "coupled" system exhibits magnetic hyperfine interactions quite different from those of the uncoupled $[Fe_3S_4]^{1+}$ cluster. We have not yet been able to assign a spin to the coupled state but some of the features of the state are reminiscent of an $S = 1$ system. The Mössbauer data suggest, but do not prove, that an extra Fe site may be present that shuttles between low-spin Fe(III) and low-spin Fe(II) with $E_m = +150$ mV. The Fe(III) may be located between the Ni(III) and the Fe_3S_4 cluster enabling it to mediate the interaction between the cluster and the Ni site. In this picture, the Fe(III) site is part of the coupled state that gives rise to signal 2. Other possibilities for signal 2 involve a ligand-based oxidation of the $[Fe_3S_4]^{1+}$ cluster or generation of a nearby radical.

Hydrogenases catalyze the reversible reaction $H_2 \leftrightarrow 2H^+ + 2e^-$ and are functional in the metabolism of a large variety of microorganisms. At present, two classes of hydrogenases are known: (i) enzymes containing Fe as the sole metal (Fe-hydrogenases) and (ii) enzymes containing Ni as well as Fe (Ni-hydrogenases or NiFe-hydrogenases). The properties of these enzymes have been thoroughly reviewed over the past 5 years (Fauque et al., 1988; Lancaster, 1988; Adams, 1990a,b; Albracht, 1990; Przybyla et al., 1992; Voordouw, 1992). Recently an H_2-forming enzyme was described, methylene-tetrahydromethanopterin dehydrogenase from *Methanobacterium thermoautotrophicum* (Zirngibl et al., 1992), in which no metals could be detected.

Hydrogenase from the purple-sulfur bacterium *Chromatium vinosum* (strain DSM 185), as studied over the years by the Amsterdam group, is a water-soluble protein consisting of two subunits of 62 and 32 kDa (van der Zwaan et al., 1987). In routine preparations approximately 1 mol of nickel, 11–12 mol of iron and 9 mol of acid-labile sulfur are detected per 94 kDa molecular mass. With regards to subunit composition and amino acid sequence, the *C. vinosum* hydrogenase falls into a category termed "standard" nickel hydrogenases; 24 other hydrogenases of this class have similar composition and sequence (Przybyla et al., 1992; Voordouw, 1992; Wu & Mandrand, 1993; Albracht, 1993). The well-studied *Desulfovibrio gigas* enzyme falls into this category also. These enzymes contain a conserved amino acid sequence motif D-P-C-x-x-C-x-x-H in the carboxy-terminal part of the large subunit. It is now well established that the first cysteine of this sequence is coordinated to nickel. In some enzymes, this residue is replaced by selenocysteine; EPR spectra have shown hyperfine broadening from ^{77}Se ($I = {}^1/_2$), giving direct evidence for a Ni–Se bond (He et al., 1989; Sorgenfrei et al., 1993). There are two more conserved cysteine residues in the amino-terminal part of the large subunit, but it is not known whether any of these are coordinated to nickel.

The small subunit of 17 nickel hydrogenases contains 10 conserved Cys residues (Voordouw, 1992; Wu & Mandrand, 1993; Albracht, 1993). Although the Cys patterns are not indicative of Fe–S cluster binding sites, it is presently thought that this subunit hosts all Fe–S clusters of the enzyme. Whether the two amino-terminal Cys residues of the large subunit are also involved in Fe–S cluster coordination is not known. Only the first four cysteine residues are strictly conserved in all hydrogenases. In some enzymes the last six

† This work was supported in part by the National Science Foundation DMB-9096231 (E.M.). S.P.J.A. is indebted to the Netherlands Organisation for the Advancement of Pure Research (NWO) for grants, supplied via the Netherlands Foundation of Chemical Research (SON), which enabled the purchase of the Bruker ECS 106 EPR spectrometer.

‡ Carnegie Mellon University. Fax (412) 268-1061.

§ Present address: University of Wisconsin—Milwaukee, Department of Chemistry, Milwaukee, WI 53201. Fax (414)-229-5530.

‖ University of Amsterdam. Fax (31) 20-525-5124.

⊥ Mayo Clinic and Foundation. Fax (507) 284-8386.

® Abstract published in *Advance ACS Abstracts,* April 1, 1994.

0006-2960/94/0433-4980$04.50/0

Cys residues are replaced by eight Cys residues grouped into two C-x-x-C-x-x-C-x-x-x-C patterns; such sequences are typically associated with regular cubane clusters (Alex et al., 1990; Halboth & Klein, 1992). In two enzymes the eight cysteines are missing altogether, and the sequence terminates shortly after the first four conserved Cys residues (Böhm et al., 1990; Tran-Betcke et al., 1990), indicating that the cubane clusters are not essential for hydrogen activation.

As isolated, the enzyme usually exhibits two different Ni(III) $S = {}^1/_2$ EPR signals (Albracht et al., 1983, 1984; van der Zwaan et al., 1990). Fernandez et al. (Fernandez et al., 1985, 1986) demonstrated for the *D. gigas* enzyme that these two Ni(III) signals represent two forms of oxidized enzyme that differ in their ability to activate H_2. The form with $g_{x,y,z}$ = 2.33, 2.16, 2.02 reacts readily with H_2 and is called the "ready" enzyme. The other form, with $g_{x,y,z}$ = 2.31, 2.23, 2.02, can react with H_2 only after prolonged (hours) contact with H_2 and is termed "unready". The conformations of nickel in ready and unready enzymes were designated as Ni–B and Ni–A, respectively. For the *C. vinosum* enzyme the corresponding conformations have been designated as Ni–a ($g_{x,y,z}$ = 2.34, 2.16, 2.01) and Ni–b ($g_{x,y,z}$ = 2.32, 2.24, 2.01) (Albracht et al., 1983, 1984; van der Zwaan et al., 1990). In order to avoid confusion in nomenclature, we will refer to the two nickel forms here as Ni_r for the ready enzyme and Ni_u for the unready enzyme.

Nearly all nickel hydrogenases require "reductive activation" for expression of catalytic activity (Lissolo et al., 1984; Teixeira et al., 1985). An "active" enzyme exhibits a Ni $S = {}^1/_2$ EPR signal, generally called Ni–C. In this paper we will refer to Ni in the active enzyme as Ni_a.

Even before it was known that nickel was present in the enzyme, it had been recognized (van Heerikhuizen et al., 1978, 1981) from multifrequency EPR that the $g = 2$ region of the spectra of the *C. vinosum* enzyme contained two overlapping signals; namely, a signal with true g values, well simulated as an $S = {}^1/_2$ system with $g_{x,y,z}$ = 2.018, 2.016, 2.002 and widths (x,y,z) = 0.68, 1.1, and 1.05 mT, and a complex spectrum with frequency-dependent g values. Using the ^{57}Fe-enriched enzyme (Albracht et al., 1982), it has been shown that both signals originated from Fe-containing species, presumably Fe–S clusters. Subsequently (Albracht et al., 1983, 1984), it was found that concomitant with the complex Fe–S signal, termed signal 2, spectral regions of both the Ni_r(III) and Ni_u(III) signals showed a splitting caused by interactions with a nearby paramagnet. Moreover, the spin-coupled nickel showed a large increase in spin–lattice relaxation rate, leading to lifetime broadening at temperatures above 20 K. Both the spin-coupled Ni(III) signals and signal 2 disappeared concomitantly upon addition of 2-mercaptoethanol (van Heerikhuizen et al., 1981; Albracht et al., 1984); no other signals appeared. Although the Q-band EPR spectra of the coupled $Ni_{r,u}$(III) species appeared to exhibit a simple 2-fold splitting of the corresponding uncoupled spectra, the details of the spectra of the coupled Fe–S species were not well understood (Albracht et al., 1984).

It has been noted already in 1981 (van Heerikhuizen et al., 1981) that mild reduction of the enzyme with ascorbate in the presence of mediating phenazine methosulfate leads to the conversion of the complicated frequency-dependent Fe–S spectrum into the simple frequency-independent "$g = 2.02$" Fe–S signal, now known to belong to an Fe_3S_4 cluster (see below). When the behavior of the nickel signals was followed as well, it was found that the reduction led to concomitant increases of the signals attributed to the *uncoupled* Ni(III) and the Fe–S centers; this has been interpreted as reduction-induced uncoupling of the two centers (Albracht et al., 1983). Since the apparent g values of the coupled Fe–S species in the oxidized enzyme ($g_{x,y} > 2$, $g_z < 2$) were quite different from those of the uncoupled Fe_3S_4 cluster-like species ($g_{x,y,z} > 2$), it was thought (Albracht et al., 1984) that the redox-linked coupling/decoupling event was accompanied by a drastic change in the electronic properties of the Fe_3S_4 cluster, possibly involving a $Fe_3S_4 \rightarrow Fe_4S_4$ cluster conversion. Attempts to exchange the hypothetical fourth Fe in this proposed conversion with ^{57}Fe were unsuccessful, however (Fontijn, R. D., and Albracht, S. P. J., unpublished observations). Redox-induced uncoupling was proposed to be due to reduction of the electronic link between both paramagnets, initially envisaged as a disulfide bridge (Albracht et al., 1985). Later it became clear that the redox event is probably an $n = 1$ process in the enzymes from *C. vinosum* strain D (Cammack et al., 1986), *Thiocapsa roseopersicina* (Cammack et al., 1989a,b), and *C. vinosum* DSM-185 (Coremans et al., 1992a). Also electron-spin echo envelope modulation and linear electric field effect studies of the *T. roseopersicina* enzyme (Cammack et al., 1989b) did not provide evidence for a Fe_4S_4/Fe_3S_4 cluster conversion during the coupling/uncoupling event. It was instead speculated that the coupling between the Ni(III) and the Fe_3S_4 cluster was provided by an extra Fe ion (Cammack et al., 1989a). To illuminate the coupling phenomenon, we initiated the current Mössbauer study.

The coupling phenomenon is not restricted to the *C. vinosum* enzyme. It has also been observed in nickel hydrogenases from *Thiocapsa roseopersicina* (Cammack et al., 1986, 1989a), the membrane-bound enzyme from *Alcaligenes eutrophus* H16 (Schneider et al., 1983), and the enzymes from *Paracoccus denitrificans* and *Pseudomonas pseudoflava* (Cammack et al., 1988). Cammack and co-workers (Schneider et al., 1983; Cammack et al., 1988) found that the response of these enzymes to 2-mercaptoethanol on partial reduction was very similar to that reported for the *C. vinosum* enzyme (van Heerikhuizen et al., 1978; Albracht et al., 1985). For the *D. gigas* hydrogenase, efforts to generate the coupled signal under highly oxidizing conditions have not been reported.

As a guide for the reader, we have summarized in Scheme 1 the various redox states of the *C. vinosum* enzyme. One state occurred as a mixture and is labeled as state A/B.

In the present paper we have used Mössbauer and EPR spectroscopies to identify the Fe-containing centers of the *C. vinosum* enzyme, with the particular view of illuminating the coupling/decoupling phenomenon attending the redox process at E_m(pH 8.0) = +150 mV (Coremans et al., 1992a). We will show that the enzyme contains two Fe_4S_4 clusters and one Fe_3S_4 cluster and we address the possibility for an additional Fe site. We will show that the coupling/decoupling phenomenon involves the Fe_3S_4 cluster and some as yet unidentified moiety. Using a special treatment, we have prepared an enzyme in the coupled state where the nickel site is clamped in the diamagnetic Ni(II)·CO form. We have studied the coupled state in considerable detail, but the nature of the electronic system which gives rise to the Mössbauer and EPR signatures is still not understood. We will discuss the features of various coupling models in the light of the present evidence.

MATERIAL AND METHODS

C. vinosum (strain DSM 185) was grown in a 700-L batch culture (van Heerikhuizen et al., 1981) in a medium essentially as described (Hendley, 1955; Albracht et al., 1983). Cells were harvested and the enzyme was isolated and purified as

Scheme 1: Schematic Representation of the Redox States of Nickel Hydrogenase from *C. vinosum*[a]

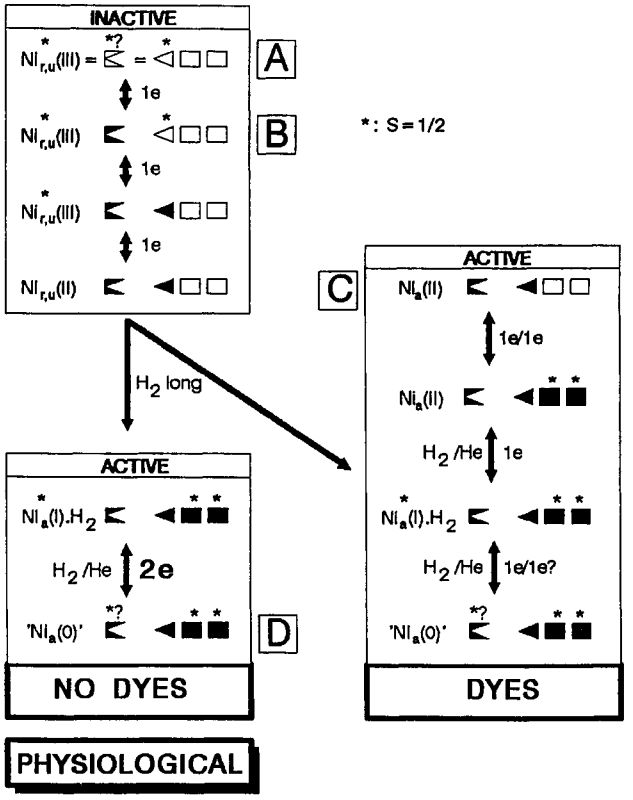

[a] After results of Coremans et al., 1992a,b, and including knowledge from the present paper. Nickel in the inactive enzyme can be either in the ready or unready form ($Ni_{r,u}$). Squares represent the Fe_4S_4 clusters; triangles stand for the Fe_3S_4 cluster; and the square missing a triangular section represents an unknown redox group. Open symbols stand for oxidized species, full symbols for reduced states. Coupling is indicated by the equivalence sign (=); $S = {}^1/_2$ systems are indicated by an asterisk. The species labeled as $Ni_a(I)\cdot(H)_2$ is also called Ni-C in the literature. The "$Ni_a(0)$" species is presumably $Ni_a(II)\cdot(H^-)_2$; this state is isoelectronic to $Ni_a(0)\cdot H_2$. Spin state and EPR properties of the unknown redox species in the oxidized state are discussed below. Note that the active enzyme responds differently to variations in the partial pressure of H_2 when redox dyes are present. Note also that there is no redox equilibrium between $Ni_{r,u}(III)$ and $Ni_a(II)$, or between $Ni_{r,u}(II)$ and $Ni_a(I)$. A step called "reductive activation" is transforming $Ni_r(II)$ into $Ni_a(II)$; only then is further reduction of the nickel possible (Coremans et al., 1992a,b).

described (Coremans et al., 1992a). Hydrogenase activity was measured amperometrically at 30 °C and pH 8.0 with a Clark-type electrode (type YSI 5331) as described (Coremans et al., 1989).

When grown with ^{57}Fe, the final Fe concentration in the medium was 4.4 μM and the bulk salts (Na_2CO_3, etc.) had previously been passed over Chelex 100 to remove contaminating Fe. The enzyme used in this study had a specific hydrogen uptake activity of 187 μmol/min per mg. It contained 11.6 mol of Fe and 0.1 mol of Cu per Ni as determined with a Hitachi 180–80 polarized Zeeman atomic absorption spectrophotometer using the internal standard method. From Fe measurements in the medium before and after the addition of ^{57}Fe an enrichment of 85% was calculated. For Mössbauer measurements the enzyme was concentrated to about 1 mM using a Centricon concentrator. EPR measurements of the Ni(III) showed that 60% of the enzyme was in the ready form and 40% in the unready form.

S-band (4 GHz) EPR spectra were obtained with a Bruker ER 061 SR microwave bridge plus a Bruker ER 6102 SR re-entrant cavity in combination with a Varian E-line spectrometer console, a Varian 12-in. magnet plus a Varian Fieldial Mark-II power supply. A field-modulation frequency of 10 kHz was employed. EPR measurements at X-band (9 GHz) were obtained with a standard Varian E-9 EPR spectrometer or a Bruker ECS 106 EPR spectrometer, while for spectra at Q-band (35 GHz) the Varian E-9 spectrometer was used in combination with the Varian E-110 microwave bridge plus the E-266 room temperature cavity; in both cases the field-modulation frequency was 100 kHz. Cooling of the sample at X- and S-band was performed by using the helium-flow system as described by Lundin and Aasa (1972) with suitable changes for the dimensions of the cryostat at S-band. In the case of the Bruker spectrometer, an Oxford Instruments ESR 900 cryostat with an ITC4 temperature controller was used. Cooling at Q-band was as described by Albracht (1974). The magnetic field was calibrated with an AEG magnetic Field Meter. The X-band frequency was measured with a HP 5246L electronic counter, supplemented with a HP 5255A frequency converter. The frequencies at S- and Q-band were derived from the field value of the absorption of α,α′-diphenyl-β-picrylhydrazyl (DPPH). The E-line spectrometer consoles were connected to a personal computer via a 12-bit A/D converter. Simulations were carried out as has been described elsewhere (Beinert & Albracht, 1982).

Samples for Mössbauer studies were prepared as follows. State A/B: Hydrogenase as isolated was incubated with 0.5 mM DCIP[1] and 0.5 mM PMS for 20 min at 30 °C in the dark to maximize coupling. After cooling in ice, the sample was quickly passed over a Sephadex G-50 column (Penefski, 1979) to remove DCIP and PMS. Approximately 40–50% of the Fe_3S_4 clusters were found to be in the coupled state. State B: The sample of state A/B was incubated with 20 mM ascorbate (pH 6) and 0.2 mM PMS (final pH 8.0) at 20 °C until the EPR signal of the Fe_3S_4 cluster was optimal. State D: The sample of state B was quickly passed twice over a Sephadex G-50 column (Penefski, 1979) to remove ascorbate and PMS. It was then eight times evacuated and gassed with H_2 and then incubated for 30 min at 50 °C to ensure complete activation and reduction. State C: The sample of state D was thawed under H_2 and incubated for 30 min at 50 °C. It was then cooled on ice, eight times evacuated, and gassed with argon. Subsequently, an anaerobic solution of benzyl viologen was added to a final concentration of 10 mM. After 10 min at 4 °C the sample was frozen in liquid nitrogen. The redox state of the enzyme in several states was inspected by EPR either at X-band by taking a small aliquot of the sample, or at S-band using the whole Mössbauer cup. Samples were shipped between our laboratories at liquid nitrogen temperatures.

RESULTS

In the following we will show that the *C. vinosum* hydrogenase contains one Fe_3S_4 cluster and two Fe_4S_4 clusters, and that the spectra of the Fe_3S_4 cluster change dramatically in the transformation from the uncoupled to the coupled state. We first discuss those states which yield spectra from which the Fe stoichiometry, and the type of cluster present can be most directly determined.

Since the enzyme contains at least four redox groups, it is sometimes cumbersome to label the samples in an unambiguous way. We therefore use the labels state A/B, B, C, and D for the redox states listed in Table 1. At potentials above +150 mV (vs NHE) the Fe_3S_4 cluster is coupled to Ni(III). We

[1] Abbreviations: DCIP, 1,2-dichlorophenolindophenol; PMS, phenazine methosulfate.

Table 1: Redox States of Hydrogenase Studied in This Paper

state			
A/B	Ni(III)	$[Fe_3S_4]^{+} \approx 50\%$ $[Fe_xS_4]^{*} \approx 50\%$	$[Fe_4S_4]^{2+}$
B	Ni(III)	$[Fe_3S_4]^{1+}$	$[Fe_4S_4]^{2+}$
C	Ni(II)	$[Fe_3S_4]^{0}$	$[Fe_4S_4]^{2+}$
D	Ni EPR-silent	$[Fe_3S_4]^{0}$	$[Fe_4S_4]^{1+}$

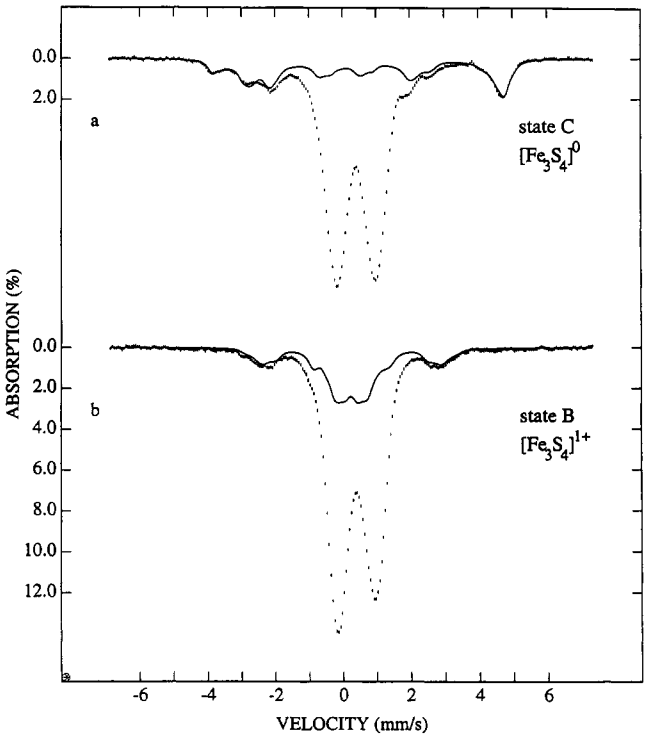

FIGURE 1: Mössbauer spectra of ^{57}Fe-enriched hydrogenase from *C. vinosum* recorded at 4.2 K in parallel fields of 1.3 T. The solid lines are theoretical spectra outlining the contributions of the Fe_3S_4 cluster in the reduced ($S = 2$) state (a) and the oxidized ($S = {}^1/_2$) state (b).

have earlier found that the complete replacement of H_2 in a reduced sample by CO leads to an EPR-silent state of Ni (van der Zwaan et al., 1986); direct proof of metal-bound CO has come from recent FTIR measurements (Bagley et al., in press). We have discovered here that in this state the nickel resists oxidation by DCIP, presumably by tight binding of CO to Ni(II). For oxidations in which the nickel site was clamped as a diamagnetic Ni(II)·CO complex, the coupling of the Fe_3S_4 cluster with the Ni site vanished at potentials above +150 mV, but it was found that the Fe_3S_4 cluster was still interacting with some paramagnetic center. We will refer to this state of the Fe_3S_4 cluster as the "coupled" state or $[Fe_xS_4]^*$, a nomenclature that allows for the possibility that some as yet unidentified additional Fe site may be involved in the coupling.

Figure 1 shows two Mössbauer spectra recorded at 4.2 K in a parallel applied field of 1.3 T. The strength of the field corresponds to the field applied when samples are studied by EPR at Q-band in the $g = 2$ region. We have recorded nearly 150 Mössbauer spectra covering the temperature range from 1.5 to 200 K in applied fields up to 8.0 T and performed extensive manipulations on these data sets using spectral simulations together with least-squares fitting of spectra exhibiting paramagnetic hyperfine structure. The spectra chosen for display will illustrate some of the characteristic features.

State C. Figure 1a shows a Mössbauer spectrum recorded of a sample in state C. Under this condition the protein is EPR-silent. The spectrum consists of a diamagnetic component, represented by the central quadrupole doublet, and a component exhibiting paramagnetic hyperfine structure in applied magnetic fields, but not in zero field. The diamagnetic component reflects eight (possibly nine, see below) iron sites with isomer shifts ranging from $\delta = 0.41$ mm/s to $\delta = 0.44$ mm/s and quadrupole splittings, $\Delta E_Q \sim 0.7$–1.5 mm/s. These parameters together with the observed diamagnetism of the sites implicate the presence of two cubane Fe_4S_4 clusters in the 2+ oxidation state.

The paramagnetic component of Figure 1a, outlined by the solid line, has features typical of those we have described previously for reduced Fe_3S_4 clusters (Papaefthymiou et al., 1987; Surerus et al., 1989; Srivastava et al., 1993). By analyzing the spectra of the entire data set recorded in this study we have obtained parameters, listed in Table 2, from which we can generate the spectra of the $[Fe_4S_4]^{2+}$ clusters in fields up to 8.0 T. By subtracting the theoretical curves of $[Fe_4S_4]^{2+}$ from the raw data we have obtained a representation of the spectra of the reduced Fe_3S_4 cluster (Figure 2).

Reduced Fe_3S_4 clusters, $[Fe_3S_4]^0$, have a ground state with electronic (cluster) spin $S = 2$. Following procedures described in detail elsewhere (Papaefthymiou et al., 1987), we have fitted the spectra of Figure 2 with the spin Hamiltonian

$$\hat{H} = D\left[S_z^2 - {}^1/_3 S(S+1) + \frac{E}{D}(S_x^2 - S_y^2)\right] + \beta \vec{H}\cdot\tilde{g}\cdot\vec{S} + \sum_{i=1}^{3}[\vec{S}\cdot\tilde{A}(i)\cdot\vec{I}(i) - g_n\beta_n\vec{H}\cdot\vec{I}(i) + \hat{H}_Q(i)] \quad (1)$$

where all symbols have their conventional meanings and where the quadrupole interactions are given by

Table 2: *C. vinosum* Hydrogenase $[[Fe_4S_4]^{2+}$ (S = 0), $[Fe_3S_4]^0$ ($S = 2$, $D = -2.8$ cm^{-1}, E/D = 0.22), and $[Fe_3S_4]^{1+}$ ($S = {}^1/_2$)]^a

cluster	site	ΔE_Q, mm/s	η	β,^{c} deg	A_x, MHz	A_y, MHz	A_z, MHz	δ,^{d} mm/s
$[Fe_4S_4]^{2+}$		0.71^b	−0.4					0.41
		0.98^b	0.1					0.42
		1.16^b	0.6					0.44
		1.49^b	0.1					0.41
$[Fe_3S_4]^0$	1	0.59(5)	0.9	65(10)	+16(2)	+17(2)	+17.4(3)	0.32(5)
	2	1.44(5)	0.9	25(5)	−22(2)	−19(2)	−16.7(3)	0.47(5)
	3	1.44(5)	0.6	10(2)	−20(2)	−25(2)	−16.6(3)	0.47(5)
$[Fe_3S_4]^{1+}$	1	−0.65	1		−38(2)	−46(2)	−47(2)	0.26
	2	0.65	0.3		+12(2)	+12(2)	+12(2)	0.26
	3	0.65	0		(+1)^e	(+1)^e	(+1)^e	0.26

^{a} The numbers in parentheses give the estimated uncertainty of the least relevant digits. ^{b} This set of parameters provides a good representation of the $[Fe_4S_4]^{2+}$ sites at all fields; however, the quoted decomposition is by no means unique. ^{c} β rotates the electric field gradient tensor into the frame of the zero field splitting tensor. ^{d} The isomer shift δ is quoted vs Fe metal at room temperature. ^{e} The A values of site 3 are undetermined but are probably $|A_i| < 5$ MHz.

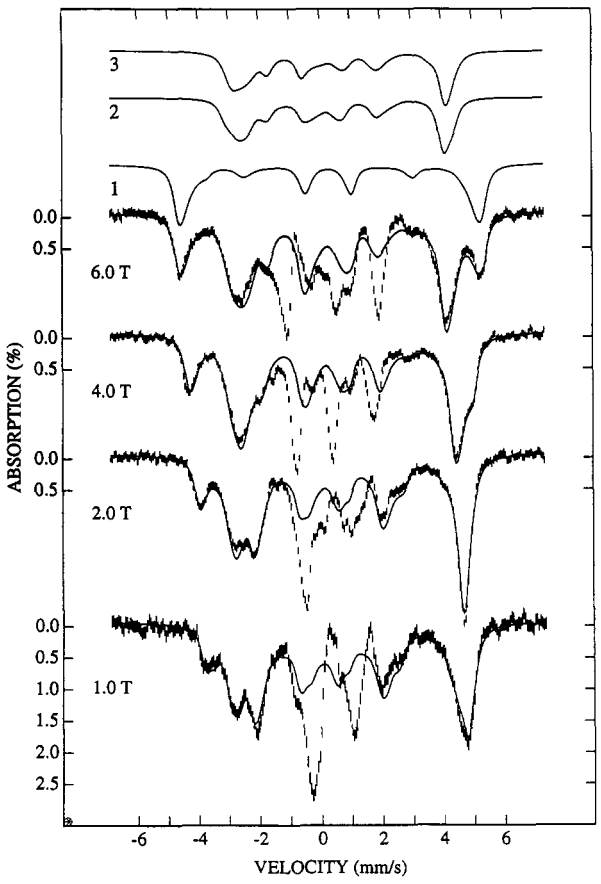

FIGURE 2: Mössbauer spectra of the $S = 2$ state of the $[Fe_3S_4]^0$ cluster recorded at 4.2 K in parallel applied fields as indicated; sample was prepared in state C. Spectra were prepared from the raw data such as shown in Figure 1a by subtracting simulated spectra representing the two $[Fe_4S_4]^{2+}$ clusters, using the parameters listed in Table 2. Solid lines are theoretical curves computed from eq 1 for $S = 2$ with the parameters of Table 2. The spectra of the three subsites are shown separately for the 6.0-T data.

$$\hat{H}_Q(i) = \frac{eQV_{\xi\xi}(i)}{12}[3I_\zeta^2(i) - I(I+1) + \eta(i)(I_\xi^2(i) - I_\psi^2(i))] \quad (2)$$

In eq 2 the subscripts (ξ, ψ, ζ) designate the principal axis system of the electric field gradient (EFG) tensor which may differ from that of the zero-field splitting tensor (principal components D and E). The results of our simulations are shown in Figure 2. Briefly, the pertinent results are as follows. The zero-field spectra of $[Fe_3S_4]^0$ consist of two quadrupole doublets with a 2:1 intensity ratio; a theoretical spectrum is shown in Figure 10a. The more intense doublet has ΔE_Q = 1.44 mm/s and δ = 0.47 mm/s and represents a valence-delocalized Fe^{2+}–Fe^{3+} pair of iron sites. The less intense doublet has $\Delta E_Q = 0.59$ mm/s and $\delta = 0.32$ mm/s and belongs to a trapped-valence Fe^{3+} site. In strong applied fields, the two sites of the delocalized pair produce slightly different spectra as indicated in the spectral decomposition shown above the 6.0-T spectrum. In all respects, the parameters obtained here are typical of those found for all $[Fe_3S_4]^0$ clusters studied thus far (Huynh et al., 1987; Papefthymiou et al., 1987; Surerus et al., 1989; Teixeira et al., 1989; Srivastava et al., 1993; Z. Hu, D. Jollie, B. Burgess, P. J. Stephens, and E. Münck, *Azotobacter vinelandii* Ferredoxin I, in preparation). In these clusters, the sites of the pair have negative magnetic hyperfine tensor components whereas the A tensor of the Fe^{3+} site has positive components. These observations are in accord with the published spin-coupling model (Papaefthymiou et al., 1987); namely, that the local spin of the Fe^{3+} site ($S_3 = {}^5/_2$) is antiparallel oriented to the system spin ($S = 2$) whereas the spin of the delocalized pair ($S_{12} = {}^9/_2$) is aligned parallel to the system spin. The solid line in Figure 1a has been drawn to represent 27% of the total absorption, suggesting that hydrogenase contains one Fe_3S_4 (27% of total Fe) and two Fe_4S_4 clusters.[2]

State B. We have also prepared a sample which has both Fe_4S_4 clusters in the 2+ state and the Fe_3S_4 cluster in the *oxidized* state, $[Fe_3S_4]^{1+}$. Oxidized Fe_3S_4 clusters have a ground state with electronic spin $S = {}^1/_2$. This state produces the $g = 2.01$ EPR signal typical for cubane $[Fe_3S_4]^{1+}$ clusters. The Mössbauer spectra of all protein-bound $[Fe_3S_4]^{1+}$ clusters studied to date have the following characteristic features (Emptage et al., 1980; Huynh et al., 1980; Kent et al., 1982; Surerus et al., 1989). First, at temperature $T \geq 50$ K the spectra consist of *one* well-defined quadrupole doublet with an isomer shift characteristic of high-spin ferric ions in a tetrahedral sulfur environment; the best studied protein, *D. gigas* Ferredoxin II, has $\Delta E_Q = 0.53$ mm/s and $\delta = 0.27$ mm/s (Huynh et al., 1980). Second, at 4.2 K the three iron sites exhibit magnetic hyperfine interactions of different signs and magnitude; typical values are $A_1 \sim -40$ MHz, $A_2 \sim +15$ MHz and $|A_3| < 5$ MHz. The 1.3-T spectrum of Figure 1b, taken on a sample in state B, exhibits a central doublet identical to that seen in Figure 1a; thus, the $[Fe_4S_4]^{2+}$ clusters are in the same state in both samples. The magnetic features resolved in Figure 1b represent site 1 of the oxidized Fe_3S_4 clusters. The solid line drawn through the data was computed with the parameters of Table 2 and drawn to represent 27% of the total absorption (i.e., 3 of 11 Fe). The contributions of sites 2 and 3 are masked by the absorption of the $[Fe_4S_4]^{2+}$ clusters. In previous studies we have used difference spectra obtained by subtracting data recorded in weak transverse applied fields from those recorded in parallel fields to obtain the parameters of site 2. This procedure produced here a poorly resolved difference spectrum and was thus unsuitable. The following manipulation, however, was successful.

Figure 3g shows a 3.0-T spectrum recorded at 1.5 K. In an applied field of 3.0 T and in the limit of long spin relaxation, a spin $S = {}^1/_2$ system produces two Mössbauer spectra for each iron site. One spectrum results from the "spin-down" and a second one from the "spin-up" electronic level. The former exhibits a magnetic splitting produced by an effective magnetic field $|H_{eff}| = |H_{int} + H| = |+{}^1/_2 A/g_n\beta_n + H|$, whereas the "spin-up" level experiences a field of $|H_{eff}| = |-{}^1/_2 A/g_n\beta_n + H|$. The intensities of the two spectra are given by the appropriate Boltzmann factors. Two theoretical spectra computed for $T = 1.5$ K and 4.2 K for site 1 are shown in Figure 3a,b, respectively; at 1.5 K the "spin-up" level is not measurably populated in an applied field of 3.0 T, and the outermost lines are not present in the spectrum. Since the spectra of diamagnetic sites are independent of the temperature between 4.2 and 1.5 K, the contributions of the two $[Fe_4S_4]^{2+}$ clusters cancel when one subtracts the 4.2-K spectrum from the 1.5-K spectrum. The resulting difference spectrum then reflects the different populations of the "spin-up" and "spin-down" levels of the $S = {}^1/_2$ state of the Fe_3S_4 cluster at the two temperatures. As can be seen from inspection of the 3.0-T difference spectrum shown in Figure 3c, this procedure reveals the outermost lines of the "spin-down" component of

[2] If the enzyme has an additional Fe site as discussed below, it would contain 12 Fe and the Fe_3S_4 cluster would represent 25% of the total Fe in the sample. For a magnetic component we could not distinguish between 25% and 27%.

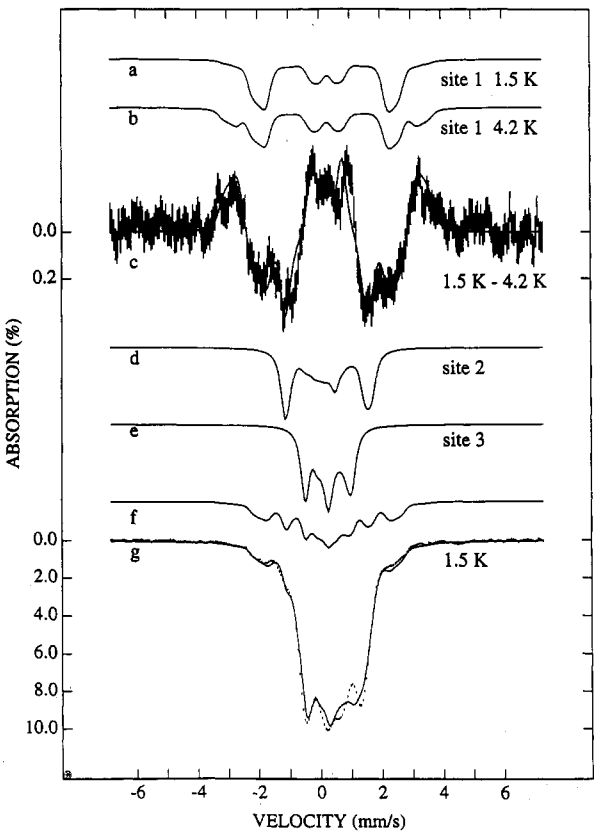

FIGURE 3: Mössbauer spectra of state B recorded in an applied field of 3.0 T at 1.5 K (g) and 4.2 K (not shown). The spectrum in c is a difference spectrum obtained by subtracting the 4.2 K data from the spectrum shown in g. The solid lines are theoretical spectra of the subsites of the Fe_3S_4 cluster computed with T = 1.5 K (a, d, e) and 4.2 K (b). The spectra in f is the sum of the spectra of the three sites normalized to represent 27% of the total absorption. The solid line in g is a theoretical spectrum representing the Fe_3S_4 and Fe_4S_4 clusters using the parameters of Table 2.

site 2, yielding a magnetic hyperfine constant $A_2 \sim +12$ MHz; a theoretical spectrum for site 2 is shown in Figure 3d. Site 3 of the Fe_3S_4 cluster exhibits only very small magnetic hyperfine interactions and cannot be resolved by taking difference spectra.

At temperatures above 50 K, the relaxation of the $S = {}^1/_2$ system is fast compared to the nuclear precession frequencies, and thus, only quadrupole doublets are observed. As observed for other Fe_3S_4 clusters, the ΔE_Q and δ values of the three sites are the same. Analysis of the high-temperature spectra yielded a temperature-independent ΔE_Q = 0.65 mm/s and δ(50 K) = 0.26 mm/s. The results obtained here show that the electronic properties of the Fe_3S_4 cluster of the *C. vinosum* hydrogenase are essentially the same as those reported for other Fe_3S_4 clusters.

State A/B. Albracht et al. (1984) have described a state of the *C. vinosum* hydrogenase that exhibits an EPR spectrum (previously labeled "signal 2") which has the appearance reminiscent of spectra of exchange-coupled dissimilar ions.[3] Signal 2 has been shown (Albracht et al., 1984) to reflect weak exchange interactions between Ni(III) and an iron–sulfur center. We will show below that the iron–sulfur center in question is the Fe_3S_4 cluster, or more precisely, the cluster which is the Fe_3S_4 cluster at potentials below $\sim +150$ mV. As the potential is increased, the hydrogenase undergoes a reversible redox reaction with midpoint potential around +150 mV, and signal 2 develops. Unfortunately, for reasons not presently understood, only a certain fraction of a given preparation attains the state which yields signal 2; the remainder retains the Fe_3S_4 cluster in the $[Fe_3S_4]^{1+}$ state.

[3] Signal 2 refers to the Fe-associated part of the spectrum, while signal 4 refers to the split Ni spectrum.

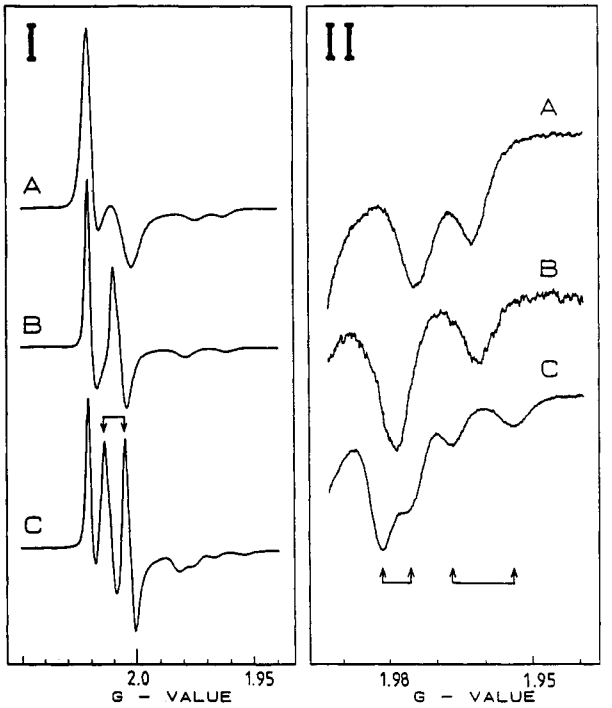

FIGURE 4: Influence of the $S = {}^1/_2$ system of Ni(III) on the EPR spectra of the coupled state A/B. A sample of *C. vinosum* hydrogenase, containing ^{57}Fe in natural abundance (2%), was 8 times evacuated and exposed to H_2 and then incubated for 30 min at 50 °C in a Thunberg-type Q-band EPR tube. After cooling to 4 °C, H_2 was replaced by CO by repeated (8 times) evacuation and exposure to gas. After 30 min under CO at 25 °C, excess DCIP was added from a side arm (final concentration 30 mM). After further incubation for 30 min at 50 °C, the sample was frozen. EPR spectra were recorded at X-band (traces A) and Q-band (traces B). No signals were observed in the spectral region where the Ni(III) signals appear. Traces C show a spectrum from a sample (different preparation) containing nickel as Ni(III). EPR conditions: microwave frequency, 9.2765 GHz (A), 35.100 GHz (B), and 35.251 GHz (C); temperature, 14 K (A), 21 K (B), and 16 K (C); microwave power, 2.0 mW (A), 2.5 mW (B), and 2.0 mW (C); modulation amplitude, 0.63 mT (A, B) and 1.25 mT (C). Spectra are plotted on the same g scale. The right-hand part (panel II) of the figure represents details of the high-field part of the spectra in panel I. Splittings due to the interacting Ni(III) and $[Fe_xS_4]^*$ systems are indicated with arrows.

On the basis of the previous studies, it is clear that signal 2 exhibits a weak exchange (or perhaps dipolar) interaction between Ni(III) and an iron–sulfur cluster. It now appears that the $S = {}^1/_2$ state of the Ni(III) produces a weak perturbation which affects the shape of signal 2, but not its basic EPR parameters, in a rather noticeable way. This perturbation has masked some rather pronounced changes involving the Fe_3S_4 cluster. These changes are quite obvious in the Mössbauer spectra. In fact, the changes are so profound that we wonder whether the cluster is still in the "standard" Fe_3S_4 conformation. We will label the modified cluster state as $[Fe_xS_4]^*$.

During the course of this study we have learned that the EPR spectra of the $[Fe_xS_4]^*$ state can be studied in more detail if the Ni site is clamped with carbon monoxide to yield the diamagnetic Ni(II)·CO state. The potential of the Ni·CO complex is sufficiently high so that the Ni site remains in the Ni(II)·CO state at potentials where signal 2 develops. Figure 4 shows X- and Q-band EPR spectra of samples prepared

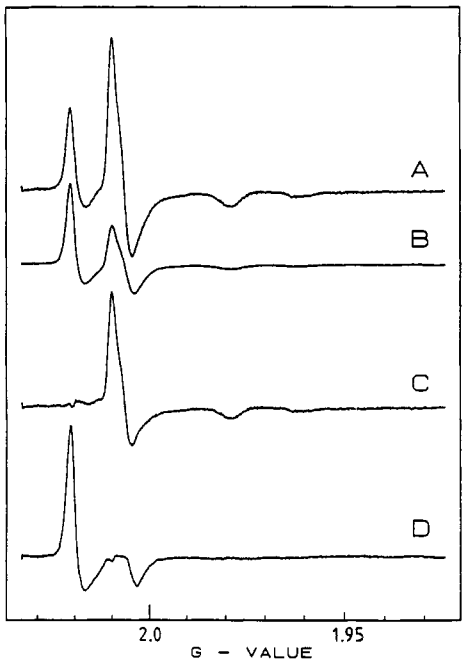

FIGURE 5: Q-band EPR spectra of the coupled state in two hydrogenase preparations with greatly different ratios of the coupled and uncoupled states. Samples were prepared as described in the legend to Figure 4, traces A and B. The preparation used for A happened to contain more coupled enzyme than the preparation used for B (same as trace B of Figure 4). Trace C is a difference (A minus B) in which the contribution of the $[Fe_3S_4]^{1+}$ cluster vanished; it shows the features of the $[Fe_xS_4]^*$ species only. Trace d is a difference (B minus A) such that the contribution of the $[Fe_xS_4]^*$ vanished; it shows the line shape of the $[Fe_3S_4]^{1+}$ cluster (compare with Figure 3b, trace D of Albracht et al. (1984)). EPR conditions for A: microwave frequency, 34.821 GHz; temperature, 19 K; microwave power, 2.0 mW; modulation amplitude, 1.25 mT. The conditions for B are described in the legend to Figure 4, trace B. Spectra were converted to the same (34.821 GHz) microwave frequency.

with Ni(II)·CO present or with the nickel site in the Ni(III) state. Comparison of the Q-band spectra in B and C shows that the complicating features of the weak interactions between Ni(III) and the iron–sulfur cluster have vanished, unmasking the signal of the state $[Fe_xS_4]^*$; only the $g \approx 2$ region is displayed in Figure 4. The low-field feature in Figure 4I reflects the $g = 2.02$ signal of the remaining $[Fe_3S_4]^{1+}$ cluster. The other features, namely the derivative features at $g = 2.01$ and the two features at $g = 1.974$ and $g = 1.963$ (at X-band), belong to the state $[Fe_xS_4]^*$. Presently, it is not clear to us whether the $g = 1.974$ and 1.963 resonances belong to one electronic system or whether they belong to two similar species of a heterogeneous state. It can be seen that the high-field resonances are field-dependent. Thus, the $g = 1.974$ resonance shifts to $g = 1.978$ at the Q-band. The details of the shift of the $g = 1.963$ resonance are less clear; it seems to move to $g = 1.961$ at the Q-band. These shifts indicate low-lying electronic states which are mixed by the magnetic field with the levels which give rise to the observed resonances. This observation rules out the possibility that the signals result from an $S = {}^1/_2$ state that is well separated in energy from excited states. Figure 5 shows the spectra of two enzyme preparations (traces A and B) with a marked difference in the fraction of coupled material. These spectra clearly show that the low-field feature from the Fe_3S_4 cluster does not belong to the spectrum of the $[Fe_xS_4]^*$ species. The difference spectra show the line shapes of the $[Fe_xS_4]^*$ species (trace C) and the Fe_3S_4 cluster (trace D) separately.

Single integrations of the X-band spectra in the forward or reverse direction showed no irregularities, i.e., the integrated

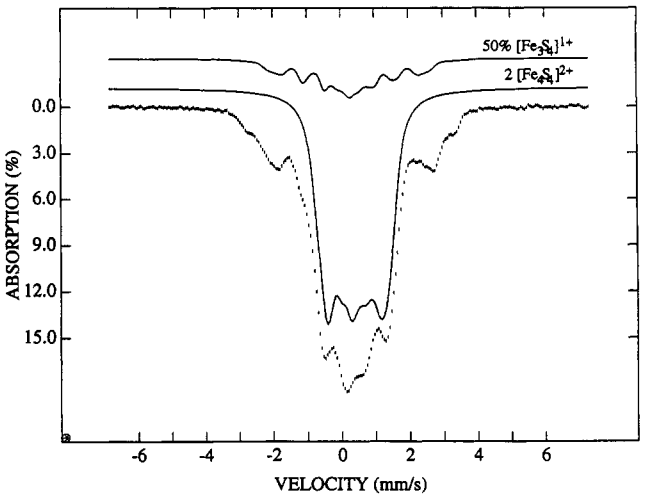

FIGURE 6: Mössbauer spectrum of state A/B recorded at 1.5 K in a parallel field of 3.0 T. The solid lines are theoretical spectra indicating the contributions of sites 1 and 2 of the $[Fe_3S_4]^{1+}$ clusters, drawn to represent 9% of the total absorption, and the two $[Fe_4S_4]^{2+}$ clusters (73%).

spectra returned to the baseline. This makes it unlikely that the spectrum extends beyond the region shown in Figure 4.

We have studied three samples containing the state $[Fe_xS_4]^*$ with Mössbauer spectroscopy. For applied fields > 0.04 T the spectra of the Ni(III)- and Ni(II)·CO-containing forms were found to be identical in the essential features.[4] We have studied many spectra of a Ni(III)-containing sample, and in the following we will present the spectra of this particular sample.

We have recorded Mössbauer spectra of state A/B in the temperature range from 1.5 to 153 K; at $T \leq 4.2$ K we have studied the sample in zero-field and applied fields of 0.05, 0.3, 1.3, 2.0, 3.0, 4.0, 5.0, and 6.0 T. A representative spectrum recorded at 1.5 K in a parallel field of 3.0 T is shown in Figure 6. Comparison of the spectra of state A/B with those obtained in states B and C shows that the two $[Fe_4S_4]$ clusters are in the same state as observed in the states that gave rise to the spectra of Figure 1a,b. A spectral simulation of the 3.0-T spectrum of the two $[Fe_4S_4]^{2+}$ clusters, based on analyses of the entire data set, is shown by the solid line in Figure 6. As pointed out above, analysis of the EPR spectra taken on the sample for the Mössbauer study indicates that approximately 50% of the $[Fe_3S_4]$ clusters have remained in the $[Fe_3S_4]^{1+}$ state. This is consistent with our understanding of the Mössbauer spectra of state A/B. Figure 6 shows also theoretical spectra of the contributions of sites 1 and 2 (using the parameters of Table 2) plotted such that they represent 50% of the original $[Fe_3S_4]^{1+}$ cluster. (We have omitted the spectrum of site 3 because its shape is not well enough known). It can be seen that the experimental spectrum contains magnetic features not attributable to the remnant $[Fe_3S_4]^{1+}$ cluster or to the two $[Fe_4S_4]^{2+}$ clusters. Figures 7 and 8 show spectra prepared from the raw data by subtracting the theoretical spectra of the two $[Fe_4S_4]^{2+}$ clusters (73% of total

[4] If the $[Fe_xS_4]^*$ is coupled to the Ni(III) site with an interaction constant of 6 mT as indicated by EPR, the $[Fe_xS_4]^*$ moiety will be decoupled in applied fields > 40 mT and the Mössbauer spectra of $[Fe_xS_4]^*$ should be the same whether the sample contains Ni(III) or Ni(II)·CO. We have studied the two Ni(II)·CO-containing samples with Mössbauer spectroscopy. Although all spectroscopic components yielded spectra for Fe_3S_4 and Fe_4S_4 essentially identical to those of the Ni(III)-containing sample, the two CO-treated samples each contained ca. 10% adventitiously bound Fe^{3+}; for this reason we have focused on the Ni(III)-containing sample.

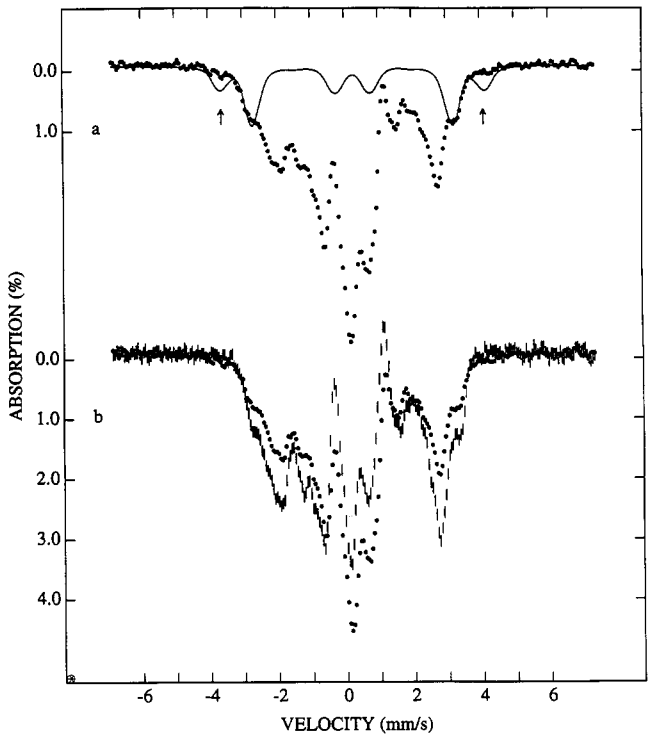

FIGURE 7: Mössbauer spectra of $[Fe_xS_4]^*$ at 4.2 K (full circles; a and b) and 1.5 K (hash marks; b) in a parallel field of 3.0 T. The spectra were prepared from the raw data by subtracting the contributions of the $[Fe_4S_4]^{2+}$ and the remnant $[Fe_3S_4]^{1+}$ clusters as described in the text. The solid line in a is a spectral simulation for site 1 under the assumption that $S = {}^1/_2$ and $\mathbf{g} = (2.0, 2.0, 2.0)$. The arrows indicate the outer lines of the "spin-up" component of the presumed system.

^{57}Fe) and the spectra of sites 1 and 2 of the remaining $[Fe_3S_4]^{1+}$ cluster (9% of total ^{57}Fe). The remainder should give the contribution of $[Fe_xS_4]^*$ and site 3 of the original $[Fe_3S_4]^{1+}$ cluster. Because of the substantial subtractions, the spectral features in the velocity range -1.5 mm/s $< v < +2.0$ mm/s are, of course, severely distorted and should thus be ignored. However, on the basis of the study of the trends through the whole data set, we believe that the velocity ranges $v > +2.0$ mm/s and $v < -1.5$ mm/s give a reasonably faithful spectral representation of $[Fe_xS_4]^*$.

In the following we describe in some detail our observations regarding $[Fe_xS_4]^*$. We have explored a variety of physical models, but thus far we have not been able to explain all observations consistently in one model. Some of our observations can be described reasonably well with an $S = 1$ spin Hamiltonian, and for ease of communication, we have performed spectral simulations under conditions such that the parameters obtained can easily be transferred to other models.

The Mössbauer spectra of $[Fe_xS_4]^*$ exhibit at least three distinguishable subcomponents which we have indicated in Figure 8a. Site 1 has the largest hyperfine splitting, corresponding to the internal magnetic field at the nucleus, $|H_{int}| = 20.4$ T. As can be seen from inspection of the spectra of Figure 8, the splitting of site 1 decreases with increasing applied field; hence $H_{int}(1) < 0$. A second spectral component moves outward with increasing field and has therefore $H_{int} > 0$. Its intensity is approximately twice that of site 1, and we thus assign sites 2 and 3 to this component. The internal field observed for site 1 is noticeably larger than the largest ($H_{int} = -16.0$ T) reported for an $[Fe_3S_4]^{1+}$ cluster.

Figure 7b shows two spectra prepared from data taken at 1.5 and 4.2 K in applied fields of 3.0 T. It can be seen that

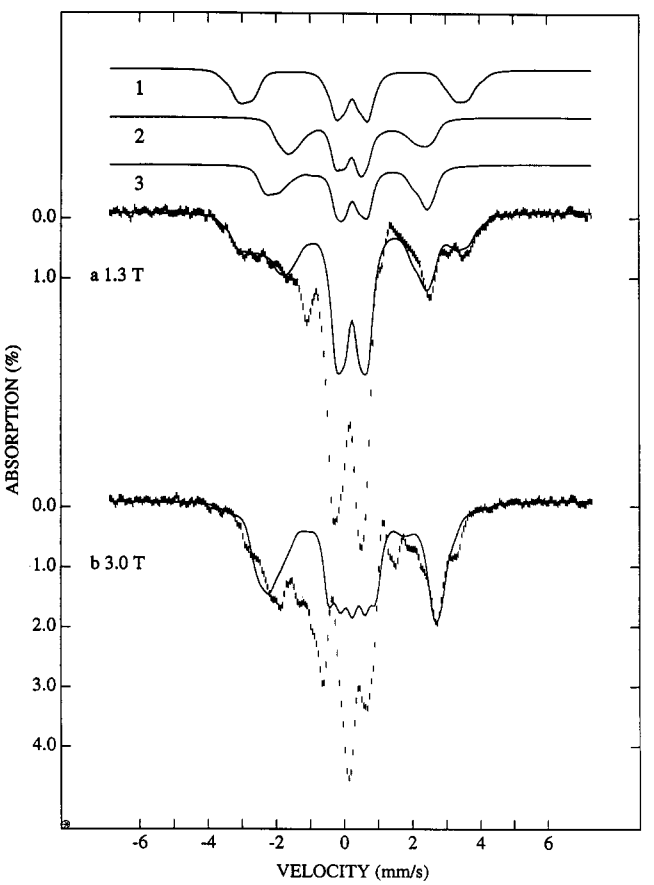

FIGURE 8: Mössbauer spectra illustrating the spectral behavior of $[Fe_xS_4]^*$. Original spectra such as that shown in Figure 6 were recorded at 4.2 K for the applied fields indicated. The contribution of the two $[Fe_4S_4]^{2+}$ clusters (73%) and the contributions of sites 1 and 2 (9% total) of the remnant $[Fe_3S_4]^{1+}$ cluster were subtracted. Because the spectrum of site 3 of the $[Fe_3S_4]^{1+}$ cluster is not well-known, its contribution has not been subtracted; it is confined to the velocity range between -1 and 1 mm/s. The solid lines are theoretical spectra illuminating the behavior of the three sites of $[Fe_xS_4]^*$. The 1.3-T spectrum was simulated for an $S = 1$ system with $D = 0$ and $g = 2.0$ using the following parameters: $\Delta E_Q = 0.65$ mm/s and $\delta = 0.26$ mm/s for all sites; $\eta = -0.6$ and $\mathbf{A} = (-29.5, -24, -29.5)$ MHz for site 1; $\eta = -0.6$ and $\mathbf{A} = (+9, +17, +17)$ MHz for site 2; $\eta = 1$ and $\mathbf{A} = (+19, +19, +13)$ for site 3. For the simulations of the 3.0-T spectrum the A values were reduced by $\approx$5%. As a model-independent quantity the reader may use the internal field of the lowest level, $H_{int}(j) = A_j/g_n\beta_n$ for each site j.

the intensities of the bands at $v > +2.0$ mm/s and $v < -1.5$ mm/s increase as the temperature is lowered to 1.5 K; this is accompanied by an intensity decrease in the center of the spectrum. These observations indicate a repopulation of electronic levels when the temperature is lowered from 4.2 to 1.5 K. (The excited state(s) must contribute a Mössbauer spectrum with substantially smaller splittings.) The presence of low-lying ($\sim$4 K) electronic levels is consistent with the observation of field-dependent g values by EPR.[5]

It is noteworthy that the intensity of *all three* spectral components increases at 1.5 K, suggesting that they all belong to the same electronic system. As shown above, the EPR spectra of $[Fe_xS_4]^*$ exhibit g values near $g = 2.0$. We can demonstrate that the Mössbauer spectrum of site 1 cannot result from a spin $S = {}^1/_2$ system with $g_x \approx g_y \approx g_z \approx 2$. The

[5] The reader might suspect that the intensity change observed at 1.5 K could be attributed to a change in the electronic relaxation rate between 4.2 and 1.5 K. This argument can be eliminated by the observation that the 45-mT spectra observed at 16 and 4.2 K are identical, suggesting that the sample is in the long relaxation limit at 4.2 K.

argument is as follows: the "spin-up" and "spin-down" states of an $S = {}^1/_2$ system produce internal magnetic fields of equal magnitude but opposite sign; specifically, $H_{int} = \pm{}^1/_2 A/g_n\beta_n$ where the + sign refers to the "spin-down" level. In the language of an $S = {}^1/_2$ spin Hamiltonian, an applied field affects the system in two ways. First, it splits the electronic levels by $\Delta E = g\beta H$. At 4.2 K and for $H = 3.0$ T, the splitting is such that the population of the "spin-up" level is 28% for $g = 2.0$. Second, the applied field adds to the internal field, H_{int}, to give an effective field at the nucleus, $H_{eff} = H_{int} + H$. For the experimental conditions of Figure 7a, the magnetic splitting of the "spin-up" state should be 2×3.0 T (twice the nuclear Zeeman term) larger than that of the "spin-down" state, and thus, the two spectra would be well separated. The solid line drawn through the spectrum is an $S = {}^1/_2$ simulation for site 1 using $g = 2$. Marked by the arrows are the outermost lines of the "spin-up" spectrum (28% population). Clearly, the spin-up component is missing from the experimental data, and the system, therefore, cannot have $S = {}^1/_2$ and $g = 2$. In fact, for $g_z \approx 2$ and for reasonably isotropic A values, the other two components of the **g** tensor would have to have values > 4 to sufficiently suppress the "spin-up" component of an $S = {}^1/_2$ system.

In order to characterize the three "resolved" sites of $[Fe_xS_4]^*$ we have performed spectral simulations using eq 1 for $S = 1$, $D = 0$, and **g** = (2.0, 2.0, 2.0). For $D = 0$, the expectation values of the electronic spin along the applied field are ± 1 and 0 for the three levels, and the internal field for the lowest state is given by $H_{int,j}(i) = A_j(i)/g_n\beta_n$ where i refers to the site and $j = x, y, z$. By choosing $D = 0$ one achieves that H_{int} attains its maximum value already in applied fields as weak as 0.05 mT. The simulations shown in Figure 8 show that the magnitudes of H_{int} of sites 2 and 3 (the spectra of site 1 lack sufficient resolution above 2.0 T) actually *decrease* by about 5% as the applied field is increased from 1.3 to 3.0 T, and another 10% as the field is raised to 6.0 T (data not shown). Thus, in order to match the theory with the splittings of Figure 8, the A values needed to be reduced with increasing field. Such reductions are an indication of the presence of low-lying excited states outside the spin manifold, here $S = 1$, used for the simulations. It should be noted that our failure to simulate the spectra with fixed A values cannot be attributed to our choice $D = 0$; in fact, for $D \neq 0$ the internal fields would *increase* with increasing field.

The caption of Figure 8 lists the parameters used for the simulations of the 1.5-T spectrum. Because of the limited resolution and the uncertainties resulting from subtracting the contributions of the other clusters, the listed parameters are, at best, approximate. In particular, the sign of the ΔE_Q and the values of η should not be taken too literally. The average A values and the trend to smaller A values with increasing field are reasonably certain. The simulations to the 1.3-T spectrum are quite good. The reader may wonder, however, why we want to reduce the A values for the 3.0-T spectrum of Figure 8b where the theory clearly misses the low-energy feature of the experimental data. Our high-temperature data suggest that all sites of $[Fe_xS_4]^*$ have the same ΔE_Q and δ values as the $[Fe_3S_4]^{1+}$ cluster in state B. Therefore, we have constrained the simulations for the low temperature spectra to have $\Delta E_Q = 0.65$ mm/s and $\delta = 0.26$ mm/s for all sites. This constraint makes it difficult to fit the 3.0-T spectrum to the desired accuracy. One should also consider that the "experimental" spectra of Figure 8 reflect only 18% of the original absorption and that site 3 of the uncoupled Fe_3S_4 cluster is still contained in the spectra. We

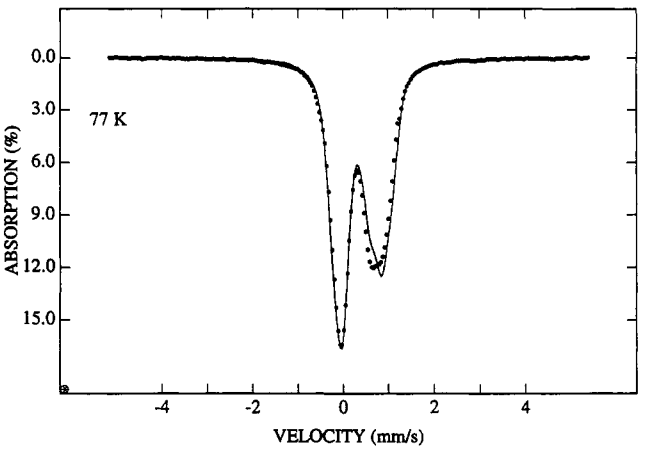

FIGURE 9: Zero-field Mössbauer spectra recorded a 77 K in state A/B (full circles) and state B (solid line).

are quite certain that although the simple $S = 1$ spin Hamiltonian can account for some features of the Mössbauer and EPR spectra, the problem is more complicated. Perhaps, the spectra reflect a coupling situation which is not adequately described by an isolated spin multiplet.

Does the Enzyme Contain an Additional Fe? It has been speculated that the *T. roseopersicina* enzyme (Cammack et al., 1989a), and hence also other enzymes showing the coupling phenomenon, might contain a monomeric Fe^{3+} site which undergoes a redox reaction concomitant with the coupling/decoupling. Is there any evidence for such a site in the Mössbauer spectra? We have seen indeed some features in the Mössbauer spectra, corresponding to 5–8% (ca. 0.5–1 Fe) of the total Mössbauer absorption, that cannot easily be attributed to the Fe_3S_4 or Fe_4S_4 clusters.

We have observed an increase in the diamagnetic fraction of the Mössbauer absorption when the protein is reduced from state A/B to state B. The change in absorption can best be illustrated by comparison of the two 77 K spectra of states A/B and B shown in Figure 9. The difference can best be described if a species with $\Delta E_Q \approx 0.6$ mm/s and $\delta \approx 0.25$ mm/s observed in state A/B and corresponding to ca. 8% of the total Fe, has changed to a state with $\Delta E_Q \approx 1.2$ mm/s and $\delta \approx 0.45$ mm/s. The low-temperature studies suggest that the latter species is diamagnetic; its parameters are compatible with assigning it to a low-spin ($S = 0$) Fe^{2+} site. This interpretation, especially the estimate of the amount of Fe involved, rests upon the assumption that the spectra of the two $[Fe_4S_4]^{2+}$ clusters are not affected, in a direct way or by a conformational change, when the system involving the Fe_3S_4 cluster is "decoupled" at $E_m = +150$ mV. If the doublet with $\Delta E_Q \approx 1.2$ mm/s reflects indeed a low-spin Fe^{2+} site, what is the oxidation and spin state of this site above +150 mV? We have searched our data for evidence of a ferric site but have obtained no conclusive evidence. On the other hand, if such a site indeed exists in a ferric state, it is likely to be part of the $[Fe_xS_4]^*$ system and thus difficult to identify. We have identified three distinct Fe sites associated with $[Fe_xS_4]^*$: we have not proven, however, that the three sites are those of the original Fe_3S_4 cluster. It is conceivable that one of the three sites belongs to a ferric site involved in $[Fe_xS_4]^*$ and that the third site of the original Fe_3S_4 cluster is hidden in the central part of the low-temperature spectra. As discussed below the fully reduced enzyme of state D may also contain evidence for an extra Fe site.

State D. Figures 10 and 11 show Mössbauer spectra of hydrogenase after reduction under 100% H_2. We have only

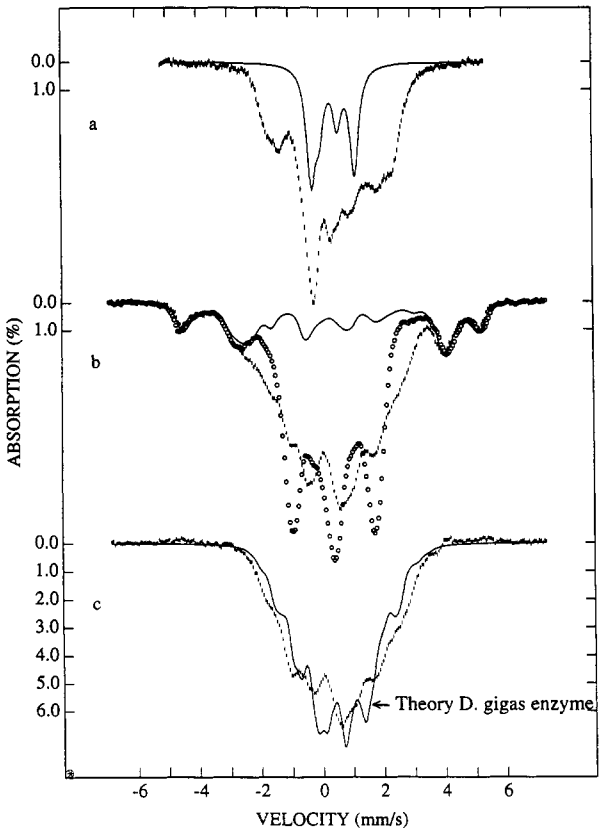

FIGURE 10: Mössbauer spectra of the reduced hydrogenase (state D) recorded at 4.2 K in zero field (a, hash marks) and an applied field of 6.0 T (b, hash marks). For comparison the corresponding spectrum of state C (open circles) is shown in b. The solid lines in a and b are theoretical spectra of the $[Fe_3S_4]^0$ cluster, drawn to represent 27% of the total absorption. The spectrum in c was obtained by subtracting the theoretical spectra of the $[Fe_3S_4]^0$ cluster from the data of b. The solid line in c is a theoretical spectrum for clusters I and II of the *D. gigas* hydrogenase, drawn to indicate the similarities of the $[Fe_4S_4]^{1+}$ clusters in both enzymes.

begun a systematic study of this state, and therefore, we report here only some preliminary results. Figure 10a,b show 4.2 K spectra recorded in zero field (a) and a parallel applied field of 6.0 T (b). Figure 10b shows also the corresponding 6.0-T spectrum of state C (open circles). It can be seen that the Fe_3S_4 cluster has remained in the $S = 2$ state after treatment with H_2. Its contribution is indicated by the theoretical curve (solid line) in Figure 10b. The spectra of Figure 10a,b show also that exposure to 100% H_2 caused reduction of the two Fe_4S_4 clusters; they are now observed in the 1+ state. The spectrum in Figure 10c was obtained by subtracting from the raw data of Figure 10b the contribution of the $[Fe_3S_4]^0$ cluster. The resulting spectrum exhibits a paramagnetic hyperfine structure similar to that observed for the hydrogenase from *D. gigas*. For comparison of the two hydrogenases we have drawn through the data a theoretical curve using the parameters that fit the *D. gigas* enzyme (This is a fit to Fe–S centers I and II according to Table IV and Figure 12 of Teixeira et al. (1989)). It is noteworthy that the Fe_4S_4 clusters of the two hydrogenases exhibit substantially smaller (30–70% for the various subsites) hyperfine splittings than those of $[Fe_4S_4]^{1+}$ clusters that yield well-resolved $g = 1.94$ features. The similarity of the hydrogenase $[Fe_4S_4]^{1+}$ clusters is also borne out by examination of the EPR spectra; both the *C. vinosum* and the *D. gigas* enzymes exhibit very broad and unresolved EPR spectra which, to date, have not been characterized in any detail.

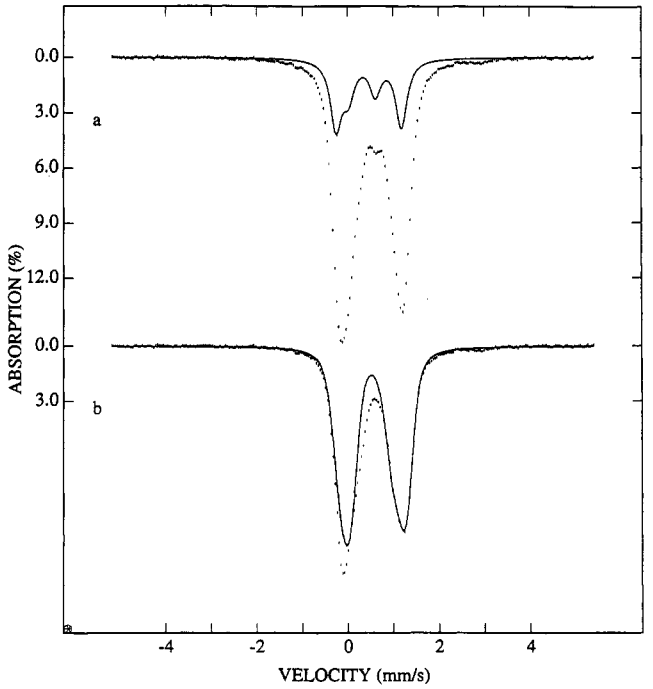

FIGURE 11: Zero-field Mössbauer spectrum (a) of state D recorded at 50 K. The solid line in a is a theoretical spectrum of the $[Fe_3S_4]^0$ cluster, computed with the parameters of Table 2. The spectrum in b was obtained by subtracting the theoretical spectrum of a from the data of a. The solid line is a superposition of two quadrupole doublets constructed in such a way that the area of the high-energy band is matched to the low-energy band. The sample contained some adventitious Fe^{2+} (<1%), barely recognizable by absorption at +2.9 mm/s Doppler velocity.

The Mössbauer spectra of reduced Fe_3S_4 clusters exhibit sharp quadrupole doublets in zero magnetic field. In order to observe the magnetic hyperfine interactions for magnetically isolated clusters, external magnetic fields have to be applied. We have added to the zero-field spectra of Figure 10a a theoretical spectrum, normalized to represent 1 cluster per molecule, of the *C. vinosum* $[Fe_3S_4]^0$ cluster, using the parameters of Table 2. It is clear to us that the spectrum of the H_2-treated sample cannot contain a contribution of the $[Fe_3S_4]^0$ cluster consisting of quadrupole doublets (subtraction of the Fe_3S_4 spectrum would yield unreasonable spectral shapes for the remainder). Thus, the spectrum of the $[Fe_3S_4]^0$ cluster must exhibit, in zero field, magnetic hyperfine interactions, implying that the cluster must be weakly coupled to another paramagnet. This coupling must be weak because uncoupled spectra of the $[Fe_3S_4]^0$ cluster are observed in applied fields > 1.0 T (see Figure 1a). One further observation is noteworthy, namely, that the 6.0-T spectrum of the $[Fe_3S_4]^0$ cluster of the H_2-reduced samples exhibits magnetic hyperfine splittings which are ca. 4% smaller than those of the corresponding spectra of state C. This suggests that the Fe_3S_4 cluster senses a conformational change of the protein resulting from the reduction of the Fe_4S_4 clusters, the Ni site or some other moiety.

Finally, we report a puzzling observation. Figure 11a shows a spectrum recorded at 50 K of the H_2-reduced sample of Figure 10. At this temperature the electronic spins of the Fe_4S_4 clusters relax fast compared to the nuclear precession frequencies and these clusters, therefore, contribute quadrupole doublets. The solid line shown in Figure 11a is a theoretical spectrum of the $[Fe_3S_4]^0$ cluster. Subtracting this theoretical spectrum from the raw data yields the spectrum of Figure 11b. If there were no other iron sites than those associated

with the two cluster types, the entire spectrum of Figure 11b would belong to the $[Fe_4S_4]^{1+}$ clusters. Now, barring asymmetries induced by texture effects (nonrandom distribution of molecules), the two absorption lines of a quadrupole doublet cover equal absorption areas (although their amplitudes and widths may differ). In Figure 11b we have constructed (solid line) a symmetric spectrum from two quadrupole doublets with $\Delta E_Q = 1.5$ mm/s, $\delta = 0.56$ mm/s and $\Delta E_Q = 1.0$ mm/s, $\delta = 0.54$ mm/s, corresponding to $^8/_{12}$ of the original absorption. It can be seen that the area of the high-energy band is covered well by the theoretical curve. Surprisingly, the low-energy band of the spectrum contains some additional absorption, corresponding roughly to 8% of the total absorption of the sample. This additional absorption would represent about 1 Fe with a surprisingly small isomer shift, namely $\delta \approx 0.05$–0.15 mm/s. We have obtained identical spectra from a sample of a different preparation, and thus, our observations are not a peculiarity of a particular sample. Moreover, the corresponding spectrum of the sample in state C containing $[Fe_3S_4]^0$ and 2 $[Fe_4S_4]^{2+}$ are entirely symmetric; the latter sample does not contain a species with $\delta \approx 0.05$–0.15 mm/s. Generation of such a species in the presence of hydrogen may offer insight into some very exciting chemistry. However, definite proof for the presence of such a species will require a coordinated effort using EPR and Mössbauer spectroscopies combined with redox titrations under H_2.

DISCUSSION

The Mössbauer studies reported here show unambiguously that *C. vinosum* hydrogenase contains one Fe_3S_4 cluster and two Fe_4S_4 clusters. In addition, the enzyme may contain an additional site with a single iron atom that can mediate an exchange coupling between the Fe_3S_4 cluster and the Ni site; we will discuss this point below. Like all Fe_4S_4 clusters studied to date, the two hydrogenase clusters are diamagnetic in the 2+ oxidation state. Both Fe_4S_4 clusters can be reduced in the presence of hydrogen into the 1+ state. However, the latter state does not exhibit the $g = 1.94$ EPR signal typical for most $[Fe_4S_4]^{1+}$ clusters. Rather, the reduced samples exhibit broad and unresolved resonances which reflect an electronic ground state somewhat different from the $g = 1.94$ state. The unusual nature of the $[Fe_4S_4]^{1+}$ state is also borne out by the Mössbauer spectra which exhibit substantially smaller magnetic hyperfine interactions than those recorded of clusters exhibiting the $g = 1.94$ signal. The Mössbauer and EPR spectral features observed here are similar to those observed by Teixeira et al. (1989) for clusters I and II of *D. gigas* hydrogenase.

At potentials below $\sim +100$ mV the Fe_3S_4 cluster of the *C. vinosum* enzyme exhibits spectral features typical of this cluster type. Thus, in the oxidized state the cluster exhibits the characteristic "$g = 2.01$" signal and the Mössbauer spectra exhibit hyperfine interactions which reflect a spin-coupled system of three antiferromagnetically coupled Fe^{3+} ions in a tetrahedral sulfide/thiolate environment. Moreover, the reduced state of the Fe_3S_4 cluster has the characteristic features of this cluster type, namely, a valence-delocalized Fe^{2+}–Fe^{3+} pair and a localized Fe^{3+} site. The fine structure as well as the hyperfine interactions are nearly identical to those reported for other Fe_3S_4 clusters. Thus, we conclude that the *C. vinosum* cluster has a cubane Fe_3S_4 core coordinated to three cysteine ligands. What, then, happens to this cluster in the oxidation process with midpoint potential around +150 mV?

As pointed out above, the redox process at $E_m \approx +150$ mV leads to a decrease of the $g = 2.02$ signal of the $[Fe_3S_4]^{1+}$ cluster with concomitant appearance of a new signal, previously termed signal 2 (Albracht et al., 1984). The amount of remaining $g = 2.02$ cluster is preparation dependent. Isotopic substitutions with ^{57}Fe as well as multifrequency EPR have shown that signal 2 involves an Fe-containing center (Albracht et al., 1982) weakly coupled (ca. 6-mT splitting) to Ni(III) (Albracht et al., 1984). We have prepared here an unperturbed coupled Fe moiety by clamping the Ni site in the diamagnetic Ni(II)·CO form. In samples thus prepared, signal 2 was still present, albeit without the perturbation introduced by the weak coupling to the Ni(III). As shown in Figure 5, signal 2 consists of a derivative-type feature at $g = 2.01$ and, at the Q-band, two absorption-type features at $g = 1.978$ and 1.961. It is presently not clear whether the resonances at $g = 1.978$ and 1.961 belong to one electronic system or whether they are the $g_\parallel$ of two species each with $g_\perp = 2.01$. Our EPR studies show that the $g = 1.978$ resonance (Q-band) is field-dependent ($g = 1.974$ at X-band). This observation suggests the presence of a low-lying electronic state which can be mixed with the ground manifold by the applied field. The $g = 1.961$ resonance seems to shift as well, albeit by a lesser amount ($g = 1.963$ at X-band). The Mössbauer studies show unambiguously that signal 2 involves the Fe_3S_4 cluster and that the $[Fe_4S_4]^{2+}$ clusters are not affected by the redox process with $E_m \approx +150$ mV. A careful examination of the isomer shifts suggests that none of the Fe sites of the Fe_3S_4 cluster is oxidized in this redox process; thus, we have no evidence that the isomer shift of any cluster site decreases. Therefore, if an electron were removed from the cluster, the redox process must be ligand-based or focused on the immediate environment (outer sphere) of the cluster. Alternatively, a radical may be generated or a monoatomic iron site, as yet not identified, may undergo a redox reaction with $E_m \approx +150$ mV. Thus far we do not understand the nature of the electronic system that gives rise to signal 2. However, since the Fe_3S_4 cluster is involved, it is important to recognize that $[Fe_3S_4]^{1+}$ clusters have low-lying electronic states which need to be considered in attempts to understand the electronic system expressed by signal 2. In the following we will discuss our results with respect to various electronic models which can be considered with the present evidence.

Mössbauer studies conducted in magnetic fields applied both parallel and perpendicular to the observed γ-radiation permit assignment of individual Mössbauer spectra to EPR-active centers (Münck, 1978). We have given evidence above that the three observed iron sites of $[Fe_xS_4]^*$ belong to the same electronic system. Due to the complexity of the present situation (less than 15% of the spectral intensity belongs to $[Fe_xS_4]^*$ and this intensity is spread over at least three iron sites), we could not conclusively prove that the Mössbauer spectra of $[Fe_xS_4]^*$ are associated with signal 2; however, spectral simulations suggest that this assumption is compatible with the data. Moreover, EPR studies with ^{57}Fe-enriched enzyme have shown that the center of signal 2 contains iron, implying the observation of a Mössbauer component exhibiting magnetic hyperfine structure. Since no other unassigned magnetic Mössbauer component has been observed, it seems reasonable to us to associate the Mössbauer spectra of $[Fe_xS_4]^*$ with signal 2.

Because the 3.0-T Mössbauer spectra of $[Fe_xS_4]^*$ lack a "spin-up" component at 4.2 K, we have argued that signal 2 cannot result from an $S = {}^1/_2$ system with $g_x \approx g_y \approx g_z \approx 2$. However, an $S = {}^1/_2$ system would be compatible with the Mössbauer data if signal 2 would extend to g values larger than $g = 4$ and the low-field portions of the signal were not detectable. While the larger Zeeman splitting of an $S = {}^1/_2$

ground state with $g_1 \approx 2$ and g_2, $g_3 > 4$ would explain the missing "spin-up" contribution, the integrated signal 2 returns reasonably well to the baseline for field $H < 3100$ G, suggesting no extension of the signal to $g > 4$. We find it difficult to ascribe signal 2 to any multiplet with $S > 1$ because the subdoublets of such multiplets generally produce doublets (or quasi-doublets for integer spin systems) with large magnetic anisotropies, unless the zero-field splittings were accidentally vanishingly small.

In the Results section we have described the Mössbauer spectra of $[Fe_xS_4]^*$, as a matter of convenience, with an $S = 1$ system. Such a system, which may result from ferromagnetic coupling of two $S = {}^1/_2$ spins, could provide a reasonable description of signal 2. Thus, an $S = 1$ multiplet with $\mathbf{g} = 2.0$ and very small zero-field splittings, $|D| < 0.01$ cm^{-1}, could account for the $g = 2.0$ resonance and for at least one of the high-field resonances. However, while spectral simulations at X-band produced reasonable simulations, we found it difficult to fit simultaneously the X-band and Q-band spectra. Moreover, the high-field Mössbauer spectra indicate that a pure $S = 1$ multiplet provides a less satisfying description of the system, as witnessed by the necessity to fit the data with field-dependent **A** tensors. Of course, field-dependent A values suggest mixing with low-lying (≤ 10 cm^{-1}) states outside the assumed $S = 1$ manifold.[6]

Signal 2 seems to result from an electronic system which results from exchange coupling of some spin (a radical or a monomeric Fe site) to the $[Fe_3S_4]^{1+}$ cluster. Before we consider this matter, some salient features of the electronic structure of $[Fe_3S_4]^{1+}$ clusters need to be discussed. Kent, Huynh, and Münck (1980) have fitted the Mössbauer data of the Fe_3S_4 cluster of *A. vinelandii* Ferredoxin I with a spin coupling model where three high-spin ferric ions ($S_1 = S_2 = S_3 = {}^5/_2$) are antiferromagnetically coupled to yield a ground state with $S = {}^1/_2$,

$$\hat{H}_{ex} = \sum_{i<j}^{3} J_{ij} \vec{S}_i \cdot \vec{S}_j \qquad (3)$$

Defining $J_{13} = J$, $J_{23} = J(1 + \epsilon)$, and $J_{12} = J(1 + \epsilon')$, analysis of the Mössbauer data showed that $0 < \epsilon < {}^3/_4$ and $\epsilon' \ll \epsilon$. For the simplified case $\epsilon' = 0$, an analytic solution to the energy levels can readily be written as

$$E = \frac{J}{2}[S(S+1) + \epsilon S_{23}(S_{23}+1)] \qquad (4)$$

The lowest multiplet of the coupled system in the state with intermediate spin $S_{23} = 2$ and system spin $S = {}^1/_2$, where $\vec{S}_{23} = \vec{S}_2 + \vec{S}_3$ and $\vec{S} = \vec{S}_1 + \vec{S}_2 + \vec{S}_3$. The first excited state at energy $3\epsilon J$ has intermediate spin $S_{23} = 3$ and system spin $S' = {}^1/_2$. Bertrand and co-workers have deduced from EPR relaxation and lineshape analyses of a series of proteins that $J \approx 40$ cm^{-1} and $\epsilon \approx 0.2$ (Gayda et al., 1982, 1983; Bertrand et al., 1984; Guigliarelli et al., 1986a,b). This places the $S' = {}^1/_2$ doublet about 25 cm^{-1} above the ground multiplet. The same parameters place four $S = {}^3/_2$ excited multiplets at 50–100 cm^{-1}. This small value of J, however, is in severe conflict with SQUID magnetometry studies by Day et al. (1988) and NMR studies by Macedo et al. (1993) which favor $J > 200$ cm^{-1}. The analyses of the low temperature Mössbauer spectra of a variety of $[Fe_3S_4]^{1+}$ ferredoxins have revealed substantial anisotropies of the ^{57}Fe magnetic hyperfine interactions (Emptage et al., 1980; Huynh et al., 1980; Kent et al., 1982; Surerus et al., 1989). These observations are unusual for high-spin ferric ions but could be rationalized with the model of Bertrand et al. (Gayda et al., 1982, 1983; Bertrand et al., 1984; Guigliarelli et al., 1986a,b; V. Papaefthymiou & E. Münck unpublished results) through mixing of electronic multiplets by zero field splitting interactions, provided that $J \leq 50$ cm^{-1}. Clearly, the electronic structure of $[Fe_3S_4]^{1+}$ clusters needs to be studied in more detail.

In considering the state of signal 2, let us assume that a spin S_R of a radical or perhaps that of a mononuclear iron site, is coupled through some exchange pathway to one iron site, say site 1, of the Fe_3S_4 cluster. This will add an additional exchange term $jS_R \cdot S_1$ to H_{ex}. If $|j|$ is small compared to the energy separation $\Delta = 3\epsilon J$ between the $S = {}^1/_2$ and $S' = {}^1/_2$ states of the cluster, we may consider only the ground doublet and rewrite the coupling term, through the use of the Wigner–Eckart theorem, as $j'S_R \cdot S$ where j' is an effective coupling constant and S the cluster spin. For $|j| \ll \Delta$, the system would become decoupled in the presence of an 8.0-T applied field, and the Mössbauer spectra of $[Fe_xS_4]^*$ would be nearly identical with those of the $[Fe_3S_4]^{1+}$ cluster, in contrast to the experimental evidence. If $|j|$, on the other hand, is comparable to or larger than Δ, the coupling problem is much more complex and one will have to treat the system as a 4-spin problem. Solution of that problem will require a better understanding of the internal coupling of the $[Fe_3S_4]^{1+}$ cluster and more information about the nature of S_R.

It has been speculated that the redox group responsible for the process at $E_m \approx +150$ mV is a protein-bound Fe(III) situated between the Ni(III) and an iron–sulfur cluster (Cammack et al., 1989a). If this putative ion would undergo a transition from low-spin ($S = {}^1/_2$) Fe(III) to low-spin ($S = 0$) Fe(II) at $E_m \approx +150$ mV, one could identify $[Fe_xS_4]^*$ perhaps with an exchange-coupled Fe(III)–$[Fe_3S_4]^{1+}$ moiety. Reduction of the Fe(III) site at $E_m \approx +150$ mV would yield the diamagnetic Fe(II) site, and the $g = 2.02$ signal of the uncoupled $[Fe_3S_4]^{1+}$ cluster would be observed. This model would help to explain two observations. First, if the site of the extra Fe would only be occupied for ca. 50% of the molecules, we would understand why only half of the Fe_3S_4 clusters can be brought into the state that produces signal 2. Second, as also recently demonstrated by Asso et al. (1992) for the Ni enzyme from *D. vulgaris* Miyazaki, the $g = 2.02$ signal of the uncoupled state shows no evidence of interaction with the Ni(III) site. Using a program for simulating the EPR spectra of two $S = {}^1/_2$ species interacting by dipolar interaction, we have concluded that the Ni(III) site and the Fe_3S_4 cluster must be separated by at least 15 Å in state B. If an Fe(III) site would occupy a site between the Ni(III) and the $[Fe_3S_4]^{1+}$ cluster in the coupled state, interaction between the three $S = {}^1/_2$ systems would be responsible for the 6.0-mT interaction observed by EPR. Interestingly, if $[Fe_xS_4]^*$ would be an $S = 1$ spin system, one should see its signature in the

[6] It is generally straightforward to determine with Mössbauer spectroscopy whether an electronic system has integer (non-Kramers systems) or half-integral electronic spin. Thus, the spectra of Kramers systems exhibit magnetic hyperfine interactions at sufficiently low temperature even in zero field while non-Kramers systems generally exhibit quadrupole doublets. Recently, however, we have shown for the P-clusters of nitrogenase that an integer spin system can exhibit magnetic splittings in zero field if two electronic states are separated by an energy smaller or comparable to the magnetic hyperfine interactions (Surerus et al., 1992). The 4.2 K zero-field spectra of $[Fe_xS_4]^*$ exhibit magnetic hyperfine splittings in state A. Since in state A the Ni(III) interacts with the $[Fe_xS_4]^*$ system, this observation would suggest that the electronic system of $[Fe_xS_4]^*$ has integer spin. It may be possible to prove this suggestion if we succeed in preparing a Ni(II)·CO inhibited sample without generating adventitious Fe^{3+}.

coupled state by a careful inspection of the Ni(III) signal. Thus, interaction with an $S = 1$ system would split the Ni(III) lines into triplets rather than doublets. However, since our samples always contain uncoupled material, the center lines of these triplets would coincide with the line positions of the uncoupled Ni(III). On the other hand, the amount of uncoupled material can be obtained by quantitative analysis of the $g = 2.02$ signal of the uncoupled $[Fe_3S_4]^{1+}$ cluster. We have just begun to study this problem in a systematic way.

We have indicated above the possibility that a new doublet with $\Delta E_Q \approx 1.2$ mm/s and $\delta \approx 0.45$ mm/s appears when the sample is transformed from state A/B to state B. The quoted parameters are compatible with a low-spin Fe(II). We have also pointed out that the fully reduced enzyme of state D has a low isomer shift component, corresponding to ca. 0.5–1 Fe, that we cannot easily attribute to any of the three iron–sulfur clusters. We have searched the spectra of state A/B for the presence of low-spin Fe(III). The isomer shift of low-spin Fe(III) complexes are in the $\delta = 0.15$–0.30 mm/s range with ΔE_Q values typically larger than 2 mm/s. Our high-temperature data of state A/B excluded any doublet with $\Delta E_Q > 1.7$ mm/s. However, a few low-spin Fe(III) complexes with $\Delta E_Q < 1.7$ mm/s are known (e.g., ferricyanide and heme cyanide complexes). The **g** tensors of low-spin Fe(III) compounds can be quite anisotropic, with principal axis component g values ranging from 0 to 4. We believe that if a low-spin ferric site is coupled to the $[Fe_3S_4]^{1+}$ cluster to produce $[Fe_xS_4]^*$, its g values must be close to the spin-only value of $g = 2.0$. Sellmann and co-workers (1991) reported the EPR ($2.1 > g_i > 2.0$ at 30 K in the solid state) and Mössbauer ($\Delta E_Q = 1.67$ mm/s, $\delta = 0.29$ mm/s at 93 K) properties of Fe(III)("S_2")$_2$(PMe$_3$)$_2$ where "S_2" = 1,2-benzenedithiolate. A site with such Mössbauer and EPR properties could perhaps be accommodated in an electronic model for $[Fe_xS_4]^*$. The reader may recall that site 1 of $[Fe_xS_4]^*$ has internal fields larger than those observed in any $[Fe_3S_4]^{1+}$ cluster. Thus, it is conceivable that this site belongs to the putative extra Fe and the spectrum of site 3 of the $[Fe_3S_4]^{1+}$ cluster is hidden in the central portion of the Mössbauer spectra. However, we emphasize that although there is some indication of an extra Fe site in the *C. vinosum* enzyme, conclusive evidence will require studies specifically geared toward resolving this question.

It is unlikely that the redox process at +150 mV is associated in any direct way with the activation of H_2. It is conceivable, however, that the process has some some, as yet not recognized, physiological function. The presence of a redox component in addition to the four known metal centers is also suggested by studies of the equilibrium of H_2 with nickel hydrogenases in the absence of mediator dyes (Coremans et al., 1992b). We may speculate that if an extra Fe is involved here, then the hydrogen-activating site in nickel hydrogenases might contain a nickel as well as an iron site. The presence of a conventional Fe_3S_4 cluster is probably not required for hydrogenase activity, since this cluster type is not present in the nickel hydrogenases from *D. baculatus* (Teixeira et al., 1990) and *M. thermoautotrophicum*, strain Marburg (Albracht et al., 1982; Coremans et al., 1992b) and strain delta-H (Johnson et al., 1986). As pointed out above, we cannot yet prove the presence of an extra iron site. However, our studies as well as those of Coremans et al. (1992b) urge additional inquiries into the nature of the observed phenomena.

ACKNOWLEDGMENT

Mrs. E. C. Bouwens, Mrs. M. Veenhuizen-Vastenburg, Mr. M. Koreman, and Mr. W. Roseboom are acknowledged for expert technical assistance. We wish to thank Dr. S. Eaton for providing the computer program MENO (used for simulating EPR spectra with spin-spin interactions between two $S = {}^1/_2$ centers).

REFERENCES

Adams, M. W. W. (1990a) *FEMS Microbiol. Rev. 75*, 219–238.
Adams, M. W. W. (1990b) *Biochim. Biophys. Acta 1020*, 115–145.
Albracht, S. P. J. (1974) *J. Magn. Reson. 13*, 299–303.
Albracht, S. P. J. (1990) in *The Molecular Basis of Bacterial Metabolism* (Hauska, G., & Thauer, R., Eds.) pp 40–51, Springer Verlag, New York.
Albracht, S. P. J. (1993) *Biochim. Biophys. Acta 1144*, 221–224.
Albracht, S. P. J., Albrecht-Ellmer, K. J., Schmedding, D. J. M., & Slater, E. C. (1982) *Biochim. Biophys. Acta 681*, 330–334.
Albracht, S. P. J., Kalkman, M. L., & Slater, E. C. (1983) *Biochim. Biophys. Acta 724*, 309–316.
Albracht, S. P. J., Van der Zwaan, J. W., & Fontijn, R. D. (1984) *Biochim. Biophys. Acta 766*, 245–258.
Albracht, S. P. J., Fontijn, R. D., & van der Zwaan, J. W. (1985) *Biochim. Biophys. Acta 832*, 89–97.
Alex, L. A., Reeve, J. N., Orme-Johnson, W. H., & Walsh, C. T. (1990) *Biochemistry 29*, 7237–7244.
Asso, M., Guigliarelli, B., Yagi, T., & Bertrand, P. (1992) *Biochim. Biophys. Acta 1122*, 50–56.
Bagley, K. A., Van Garderen, C. J., Chen, M., Duin, E. C., Albracht, S. P. J., & Woodruff, W. H. (in press) *Biochemistry*.
Beinert, H., & Albracht, S. P. J. (1982) *Biochim. Biophys. Acta 683*, 245–277.
Bertrand, P., Guigliarelli, B., Meyer, J., & Gayda, J.-P. (1984) *Biochimie 66*, 77–79.
Böhm, R., Sauter, M., & Böck, A. (1990) *Mol. Microbiol. 4*, 231–243.
Cammack, R., Rao, K. K., Serra, J., & Llama, M. J. (1986) *Biochimie 68*, 93–96.
Cammack, R., Fernandez, V. M., & Schneider, K. (1988) in *Nickel in Hydrogenases from Sulfate-Reducing, Photosynthetic, and Hydrogen-Oxidizing Bacteria* (Lancaster, J. R., Jr., Ed.) pp 167–190, VCH Publishing, Inc., New York.
Cammack, R., Bagyinka, C., & Kovacs, K. L. (1989a) *Eur. J. Biochem. 182*, 357–362.
Cammack, R., Kovacs, K. L., McCracken, J., & Peisach, J. (1989b) *Eur. J. Biochem. 182*, 363–366.
Coremans, J. M. C. C., Van der Zwaan, J. W., & Albracht, S. P. J. (1989) *Biochim. Biophys. Acta 997*, 256–267.
Coremans, J. M. C. C., van der Zwaan, J. W., & Albracht, S. P. J. (1992a) *Biochim. Biophys. Acta 1119*, 157–168.
Coremans, J. M. C. C., van Garderen, C. J., & Albracht, S. P. J. (1992b) *Biochim. Biophys. Acta 1119*, 148–156.
Day, E. P., Peterson, J., Bonvoisin, J. J., Moura, I., & Moura, J. J. G. (1988) *J. Biol. Chem. 263*, 3684–3689.
Emptage, M. H., Kent, T. A., Huynh, B. H., Rawlings, J., Orme-Johnson, W. H., & Münck, E. (1980) *J. Biol. Chem. 255*, 1793–1796.
Fauque, G., Peck, H. D., Jr., Moura, J. J. G., Huynh, B. H., Berlier, Y., DerVartanian, D. V., Teixeira, M., Przybyla, A. E., Lespinat, P. A., Moura, I., & LeGall, J. (1988) *FEMS Microbiol. Rev. 54*, 299–344.
Fernandez, V. M., Hatchikian, E. C., & Cammack, R. (1985) *Biochim. Biophys. Acta 832*, 69–79.
Fernandez, V. M., Hatchikian, E. C., Patil, D. S., & Cammack, R. (1986) *Biochim. Biophys. Acta 883*, 145–154.
Gayda, J.-P., Bertrand, P., Theodule, F.-X., & Moura, J. J. G. (1982) *J. Chem. Phys. 77*, 3387–3391.
Gayda, J. P., Bertrand, P., Guigliarelli, B., & Meyer, J. (1983) *J. Chem. Phys. 79*, 5732–5733.
Guigliarelli, B., Gayda, J. P., Bertrand, P., & More, C. (1986a) *Biochim. Biophys. Acta 871*, 149–155.

Guigliarelli, B., More, C., Bertrand, P., & Gayda, J. P. (1986b) *J. Chem. Phys. 85*, 2774–2777.
Halboth, S., & Klein, A. (1992) *Mol. Gen. Genet. 233*, 217–224.
He, S. H., Teixeira, M., LeGall, J., Patil, D. S., Moura, I., Moura, J. J. G., DerVartanian, D. V., Huynh, B. H., & Peck, H. D., Jr. (1989) *J. Biol. Chem. 264*, 2678–2682.
Hendley, D. D. (1955) *J. Bacteriol. 70*, 625–634.
Huynh, B. H., Moura, J. J. G., Moura, I., Kent, T. A., LeGall, J., Xavier, A. V., & Münck, E. (1980) *J. Biol. Chem. 255*, 3242–3244.
Huynh, B. H., Patil, D. S., Moura, I., Teixeira, M., Moura, J. J. G., DerVartanian, D. V., Czechowski, M. H., Prickril, B. C., Peck, H. D., Jr., & LeGall, J. (1987) *J. Biol. Chem. 262*, 795–800.
Johnson, M. K., Zambrano, I. C., Czechowski, M. H., Peck, H. D., Jr., DerVartanian, D. V., & LeGall, J. (1986) in *Frontiers in Bioinorganic Chemistry* (Xavier, A. V., Ed.) pp 36–44, VCH Verlagsgesellschaft, Weinheim, FRG.
Kent, T. A., Huynh, B. H., & Münck, E. (1980) *Proc. Natl. Acad. Sci. U.S.A. 77*, 6574–6576.
Kent, T. A., Dreyer, J.-L., Kennedy, M. C., Huynh, B. H., Emptage, M. H., Beinert, H., & Münck, E. (1982) *Proc. Natl. Acad. Sci. U.S.A. 79*, 1096–1100.
Lancaster, J. R., Jr. (1988) *The Bioinorganic Chemistry of Nickel*, VCH Publishers, Inc., New York.
Lissolo, T., Pulvin, S., & Thomas, D. (1984) *J. Biol. Chem. 259*, 11725–11729.
Lundin, A., & Aasa, R. (1972) *J. Magn. Reson. 8*, 70–73.
Macedo, A. L., Moura, I., Moura, J. J. G., LeGall, J., & Huynh, B. H. (1993) *Inorg. Chem. 32*, 1101–1105.
Münck, E. (1978) *Methods Enzymol. 54*, 346–379.
Papaefthymiou, V., Girerd, J.-J., Moura, I., Moura, J. J. G., & Münck, E. (1987) *J. Am. Chem. Soc. 109*, 4703–4710.
Penefski, H. S. (1979) *Methods Enzymol. 56*, 527–530.
Przybyla, A. E., Robbins, J., Menon, N., & Peck, H. D., Jr. (1992) *FEMS Microbiol. Rev. 88*, 109–136.
Schneider, K., Patil, D. S., & Cammack, R. (1983) *Biochim. Biophys. Acta 748*, 353–361.
Sellmann, D., Geck, M., Knoch, F., Ritter, G., & Dengler, J. (1991) *J. Am. Chem. Soc. 113*, 3819–3828.
Sorgenfrei, O., Klein, A., & Albracht, S. P. J. (1993) *FEBS Lett. 332*, 291–297.
Srivastava, K. K. P., Surerus, K. K., Conover, R. C., Johnson, M. K., Park, J.-B., Adams, M. W. W., & Münck, E. (1993) *Inorg. Chem. 32*, 927–936.
Surerus, K. K., Kennedy, M. C., Beinert, H., & Münck, E. (1989) *Proc. Natl. Acad. Sci. U.S.A. 86*, 9846–9850.
Surerus, K. K., Hendrich, M. P., Christie, P. D., Rottgardt, D., Orme-Johnson, W. H., & Münck, E. (1992) *J. Am. Chem. Soc. 114*, 8579–8590.
Teixeira, M., Moura, I., Xavier, A. V., Huynh, B. H., DerVartanian, D. V., Peck, H. D., Jr., LeGall, J., & Moura, J. J. G. (1985) *J. Biol. Chem. 260*, 8942–8950.
Teixeira, M., Moura, I., Xavier, A. V., Moura, J. J. G., LeGall, J., DerVartanian, D. V., Peck, H. D., Jr., & Huynh, B.-H. (1989) *J. Biol. Chem. 264*, 16435–16450.
Teixeira, M., Moura, I., Fauque, G., DerVartanian, D. V., LeGall, J., Peck, H. D., Jr., Moura, J. J. G., & Huynh, B.-H. (1990) *Eur. J. Biochem. 189*, 381–386.
Tran-Betcke, A., Warnecke, U., Böcker, C., Zaborosch, C., & Friedrich, B. (1990) *Eur. J. Biochem. 189*, 381–386.
van der Zwaan, J. W., Albracht, S. P. J., Fontijn, R. D., & Roelofs, Y. B. M. (1986) *Biochim. Biophys. Acta 872*, 208–215.
van der Zwaan, J. W., Albracht, S. P. J., Fontijn, R. D., & Mul, P. (1987) *Eur. J. Biochem. 169*, 377–384.
van der Zwaan, J. W., Coremans, J. M. C. C., Bouwens, E. C. M., & Albracht, S. P. J. (1990) *Biochim. Biophys. Acta 1041*, 101–110.
van Heerikhuizen, H., Albracht, S. P. J., ten Brink, B., Evers-van Twist, L., & Slater, E. C. (1978) in *Hydrogenases: Their Catalytic Activity, Structure and Function* (Schlegel, H. G., & Schneider, K., Eds.) pp 151–158, Goltze Verlag, Göttingen.
van Heerikhuizen, H., Albracht, S. P. J., Slater, E. C., & Van Rheenen, P. S. (1981) *Biochim. Biophys. Acta 657*, 26–39.
Voordouw, G. (1992) *Adv. Inorg. Chem. 38*, 397–422.
Wu, L.-F., & Mandrand, M. A. (1993) *FEMS Microbiol. Rev. 104*, 249–270.
Zirngibl, C., Van Dongen, W., Schwörer, B., Von Bünau, R., Richter, M., Klein, A., & Thauer, R. K. (1992) *Eur. J. Biochem. 208*, 511–520.